GW Parameter Estimations and Simulations

S. Haino

Academia Sinica

Outline

- G.P.E. – GPU accelerated Parameter Estimation
- Comparison of results – GW events analysis
- Comparison of results – Simulation
- Immediate future – O3 simulation
- Physics targets – O5 simulation

Acknowledgements

- Narikawa-san, Tagoshi-san, Morisaki-san, Michimura-san
  Discussions and suggestions
- Ting-Wai Chiu (NTNU/ASIoP)
  GPU developments and his GPU farm supports
- Chun-Yu Lin (NCHC)
  National Center for High-performance Computing
- Academia Sinica Grid Center (ASGC)
  GPU farm and computing supports

Outline

- G.P.E. – GPU accelerated Parameter Estimation
- Comparison of results – GW events analysis
- Comparison of results – Simulation
- Immediate future – O3 simulation
- Physics targets – O5 simulation

Motivation

- Parameter Estimation (PE) is a time-consuming process; we need to find a new way to accelerate it in view of many-GW-detection era towards 3G
- Freq.-domain CBC PE on
  15 parameters (3(M_c,q,φ) +6(spin) +6(ext.)) with
  - Nested sampling with MCMC sub-chains and
  - *IMRPhenomPv2* waveform model
  has been accelerated with GPU
- The codes are all newly written in C++ and CUDA and produce the same output for *cbcBayesPostProc*

P.E. with Bayes' theorem

arXiv:1409.7215

Parameter estimation can then be performed using Bayes' theorem, where a prior probability distribution $p(\theta|H)$ is updated upon receiving the new data d from the experiment to give a posterior distribution $p(\theta|d,H)$,

$$p(\theta|d,H) = \frac{p(\theta|H)p(d|\theta,H)}{p(d|H)}. \tag{1}$$

Nested sampling

- Introduced by J. Skilling to compute Bayesian evidence(Z) with MCMC sub-chains by transforming the Multi-Dimensional integral into 1-dimension over the prior volume Ref(e.g.): *arXiv:1409.7215*

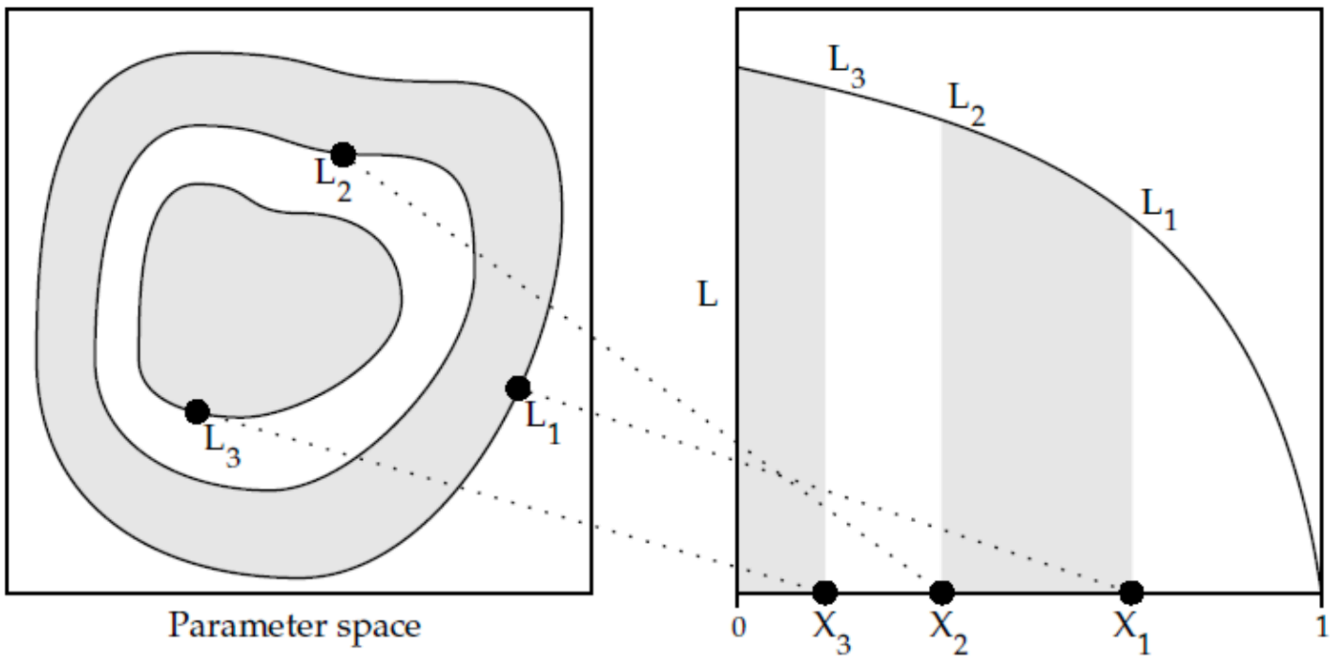

Nested sampling in LAL

- Implemented in :
  LALInferenceNest, LALInferenceNestedSampler, LALInferenceProposal, LALInferencePrior, …
- 5 methods used for Jump proposals (LAL default) :
  - *CovarianceEigenvectorJump*
  - *DifferentialEvolution*
  - *EnsembleStretch*
  - *EnsembleWalk*
  - *DistanceLikelihood*
- MCMC sub-chain length is determined at every (*Nlive*/10) iterations from autocorrelation length

For more details please refer: *arXiv:1409.7215* or the source code itself

GPU Approach

- Waveform and likelihood calculations are the dominant sources of time consumption for P.E.

  - 4,096(*srate*) x8(*seglen*)/2 x2(*Nifo*) = 32,768 /call
  - ~1,000 times called per iteration
  - ~16,000 iterations per run

  => 5 x10^{11} calculations / run

- These particular parts are implemented in CUDA
  - Single Floating point is used (10^{-5}~10^{-4} precision)

* In *LALSimulation*, waveform calculation can run in OpenMP but the performance didn't improve so significantly on Core™ i7

Core of the GPU code

cimr: IMRphenomP wave form calculation

Each GPU core : each frequency bin

```
if (xmin <= x && x < Nfr) {
  if (x < xmax) cimr(ph, hpr, hpi, hcr, hci, fr);
  int k = blockIdx.y;
  int l = k*Nfr+x;
  core(fr, dr[l], di[l], ps[l], hpr, hpi, hcr, hci,
          fp[k], fc[k], dt[k], Slen, cs[i], ss[i], rr[i], ri[i]);
}
__syncthreads();
```

core: Likelihood calculation

Core of the GPU code

Each GPU core : each frequency bin

```
STATIC inline void core(real  fr, real dtr, real dti, real psd,
                        real hpr, real hpi, real hcr, real hci,
                        real  fp, real  fc, real  dt, int slen,
                        real &cs, real &ss, real &rr, real &ri)
{
  tsft(hpr, hpi, fr*_tc); tsft(hcr, hci, fr*_tc);

  real cpr = _czp*hpr+_szp*hcr, cpi = _czp*hpi+_szp*hci;
  real ccr = _czp*hcr-_szp*hpr, cci = _czp*hci-_szp*hpi;
  real tpr =   fp*cpr+  fc*ccr, tpi =   fp*cpi+  fc*cci;
  tsft(tpr, tpi, fr*dt);

  real dT  = 1./Rsmp, dtn = 2*dT/Rsmp/slen;
  real dfr = dtr-tpr, dfi = dti-tpi, ssq = psd*dT*dT;

  cs += -dtn*(dfr*dfr+dfi*dfi)/ssq; ss += dtn*(tpr*tpr+tpi*tpi)/ssq;
  rr +=  dtn*(tpr*dtr+tpi*dti)/ssq; ri += dtn*(tpr*dti-tpi*dtr)/ssq;
}
```

Polarization and Detector antenna pattern

tpr, tpi: Waveform template

dfr, dfi: Data-template

cs: Chis-quare (log(likelihood)) element

Performance test

- GW150914 data from LIGO Open Science Center
- LAL: *lalinferene_nest* with *IMRPhenomPv2*, *seglen*=8, *Nlive*=500 are used as a reference
  - running on single CPU (4 parallel jobs / machine)

- GPE (GPU-accelerated P.E.) :
  - running on single CPU/machine and tested with 3 different GPU boards (NVIDIA™ GeForce™)
- 23 independent runs performed and time consumptions and output results are compared

Performance comparison

Code	Hardware	Spec.	Wall Time Mean ± RMS	Acceleration w.r.t. LAL	Improvement
LAL	Core™ i7	4 cores (x2 HT) 3.6 GHz	24:27:24 ± 47:42		
GPE	GeForce™ GTX 1060	1152 cores 1.76 GHz 192 bit Bus	17:21 ± 0:28	× 84.5	
GPE	GeForce™ GTX 1070	1920 cores 1.68 GHz 256 bit Bus	13:58 ± 0:17	× 105.0	24% to 1060
GPE	GeForce™ GTX 1080	2560 cores 1.85 GHz 256 bit Bus	12:25 ± 0:15	× 118.1	40% to 1060 13% to 1070

Log Bayes factors $\ln(B_{s/n})$: 254.7±0.3 and 254.5±0.3 in LAL and GPE, respectively

Nested sampling parameters

LALInference_nest

```
16000: accpt: 0.253 Nmcmc: 5000 sub_accpt: 0.331 slpy: 74.5% H: 26.18 nats logL:-31862.067 ->-31861.838 logZ: -31890.951 deltalogLmax: 285.02 dZ: 0.14
16001: accpt: 0.352 Nmcmc: 5000 sub_accpt: 0.290 slpy: 74.6% H: 26.18 nats logL:-31862.067 ->-31861.416 logZ: -31890.951 deltalogLmax: 285.02 dZ: 0.14
16002: accpt: 0.388 Nmcmc: 5000 sub_accpt: 0.259 slpy: 74.7% H: 26.18 nats logL:-31862.066 ->-31862.049 logZ: -31890.951 deltalogLmax: 285.02 dZ: 0.14
16003: accpt: 0.259 Nmcmc: 5000 sub_accpt: 0.337 slpy: 74.6% H: 26.18 nats logL:-31862.066 ->-31862.017 logZ: -31890.951 deltalogLmax: 285.02 dZ: 0.14
16004: accpt: 0.342 Nmcmc: 5000 sub_accpt: 0.291 slpy: 74.7% H: 26.18 nats logL:-31862.066 ->-31861.974 logZ: -31890.951 deltalogLmax: 285.02 dZ: 0.14
16005: accpt: 0.244 Nmcmc: 5000 sub_accpt: 0.353 slpy: 74.6% H: 26.18 nats logL:-31862.065 ->-31861.798 logZ: -31890.951 deltalogLmax: 285.02 dZ: 0.14
16006: accpt: 0.266 Nmcmc: 5000 sub_accpt: 0.330 slpy: 74.5% H: 26.18 nats logL:-31862.065 ->-31861.219 logZ: -31890.951 deltalogLmax: 285.02 dZ: 0.14
16007: accpt: 0.364 Nmcmc: 5000 sub_accpt: 0.269 slpy: 74.6% H: 26.18 nats logL:-31862.065 ->-31861.519 logZ: -31890.951 deltalogLmax: 285.02 dZ: 0.14
16008: accpt: 0.406 Nmcmc: 5000 sub_accpt: 0.259 slpy: 74.7% H: 26.18 nats logL:-31862.065 ->-31861.810 logZ: -31890.951 deltalogLmax: 285.02 dZ: 0.14
16009: accpt: 0.233 Nmcmc: 5000 sub_accpt: 0.350 slpy: 74.6% H: 26.18 nats logL:-31862.064 ->-31861.960 logZ: -31890.951 deltalogLmax: 285.02 dZ: 0.14
16010: accpt: 0.528 Nmcmc: 5000 sub_accpt: 0.190 slpy: 74.7% H: 26.18 nats logL:-31862.064 ->-31861.260 logZ: -31890.950 deltalogLmax: 285.02 dZ: 0.14
```

Accept rate Sub-accept rate Sloppy fraction dZ

GPE

```
16034: accpt: 0.205691 Nmcmc: 5000 sa: 0.373176 slf: 75.3115 H: 26.5989 lm= -31862.262 -31861.559 lZ: -31891.545 dlm: 284.651 dZ: 0.170992
16035: accpt: 0.317409 Nmcmc: 5000 sa: 0.291025 slf: 75.4115 H: 26.5991 lm= -31862.262 -31861.883 lZ: -31891.545 dlm: 284.651 dZ: 0.170659
16036: accpt: 0.373984 Nmcmc: 5000 sa: 0.253248 slf: 75.5115 H: 26.5993 lm= -31862.262 -31861.738 lZ: -31891.545 dlm: 284.651 dZ: 0.170325
16037: accpt: 0.477551 Nmcmc: 5000 sa: 0.213272 slf: 75.6115 H: 26.5995 lm= -31862.262 -31861.582 lZ: -31891.544 dlm: 284.651 dZ: 0.169994
16038: accpt: 0.246721 Nmcmc: 5000 sa: 0.336998 slf: 75.5115 H: 26.5997 lm= -31862.262 -31861.648 lZ: -31891.544 dlm: 284.651 dZ: 0.169663
16039: accpt: 0.342857 Nmcmc: 5000 sa: 0.268239 slf: 75.6115 H: 26.5999 lm= -31862.258 -31861.516 lZ: -31891.544 dlm: 284.651 dZ: 0.169332
16040: accpt: 0.336066 Nmcmc: 5000 sa: 0.277234 slf: 75.7115 H: 26.6001 lm= -31862.258 -31862.051 lZ: -31891.544 dlm: 284.651 dZ: 0.169002
16041: accpt: 0.255144 Nmcmc: 5000 sa: 0.325005 slf: 75.6115 H: 26.6003 lm= -31862.258 -31861.871 lZ: -31891.544 dlm: 284.651 dZ: 0.168675
16042: accpt: 0.309836 Nmcmc: 5000 sa: 0.293424 slf: 75.7115 H: 26.6005 lm= -31862.258 -31862.215 lZ: -31891.544 dlm: 284.651 dZ: 0.168347
16043: accpt: 0.283128 Nmcmc: 5000 sa: 0.307815 slf: 75.6115 H: 26.6007 lm= -31862.254 -31862.109 lZ: -31891.544 dlm: 284.651 dZ: 0.168018
```

Accept rate Sub-accept rate Sloppy fraction dZ

For more details please refer: *arXiv:1409.7215* or the source code itself

Comparisons (Nested sampling parameters)

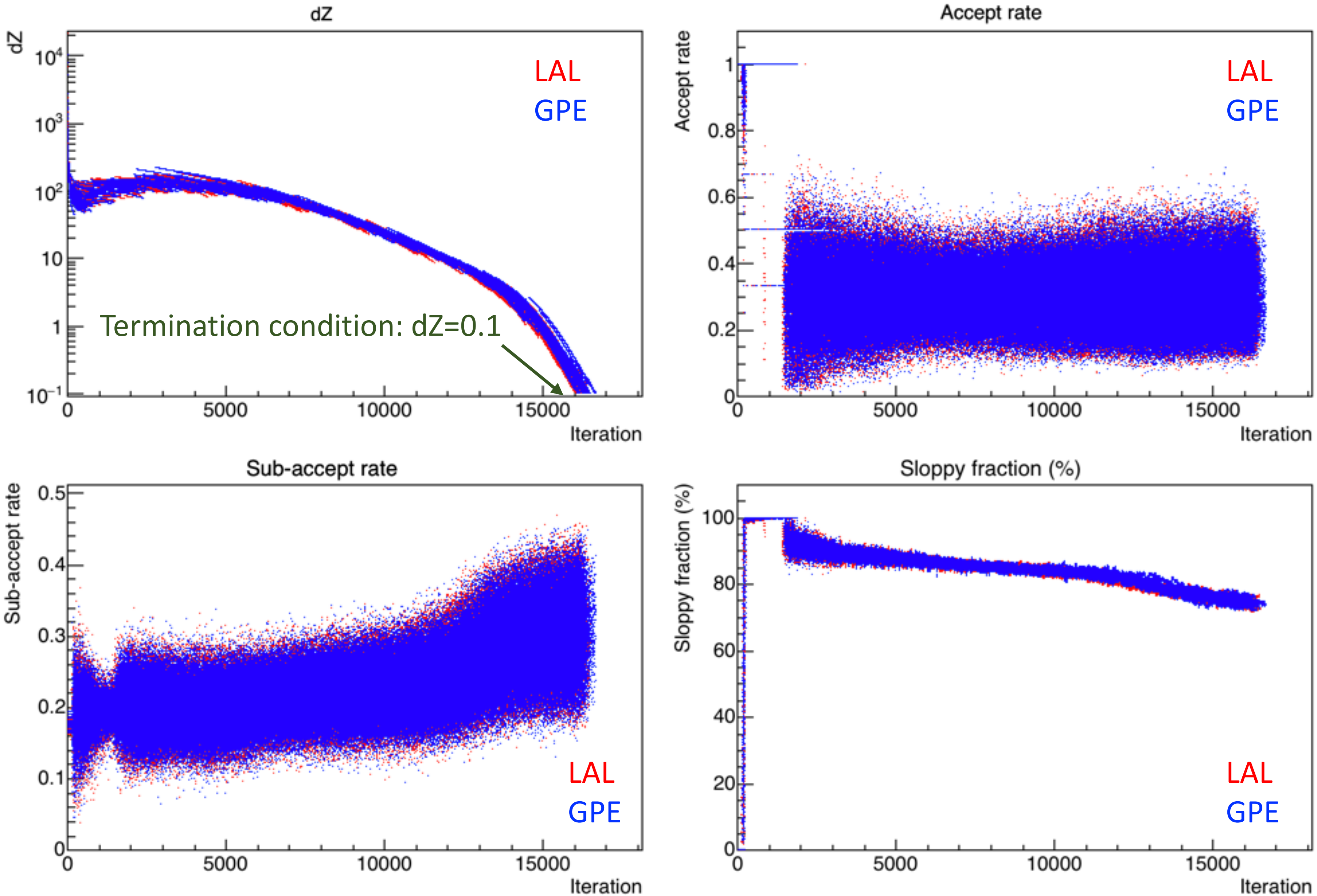

Comparisons (CBC intrinsic parameters)

Parameters in the final 500 live points (from 23 independent runs)

Note: they are not the posterior distributions

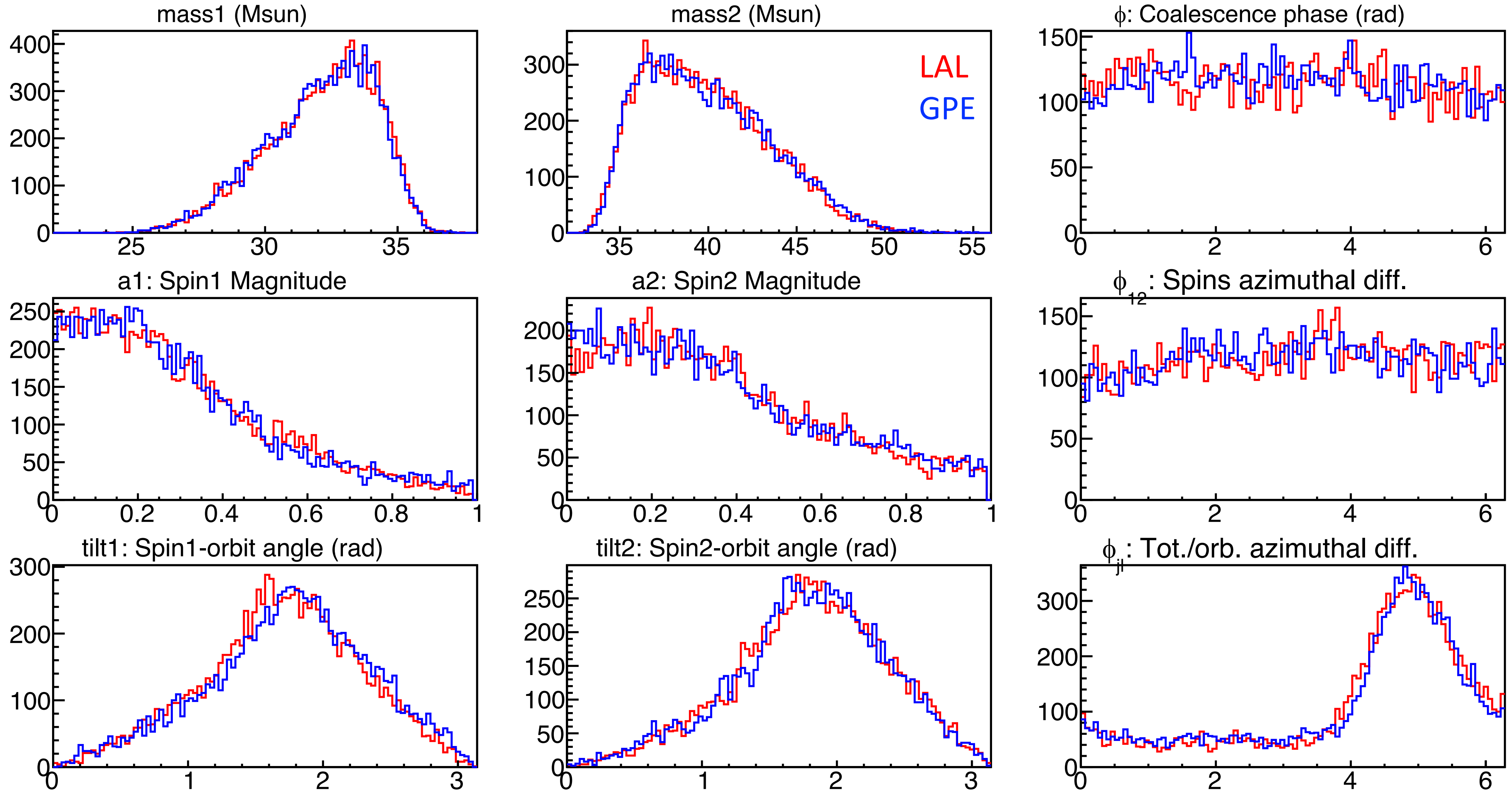

Comparisons (CBC extrinsic parameters)

Parameters in the final 500 live points (from 23 independent runs)

Note: they are not the posterior distributions

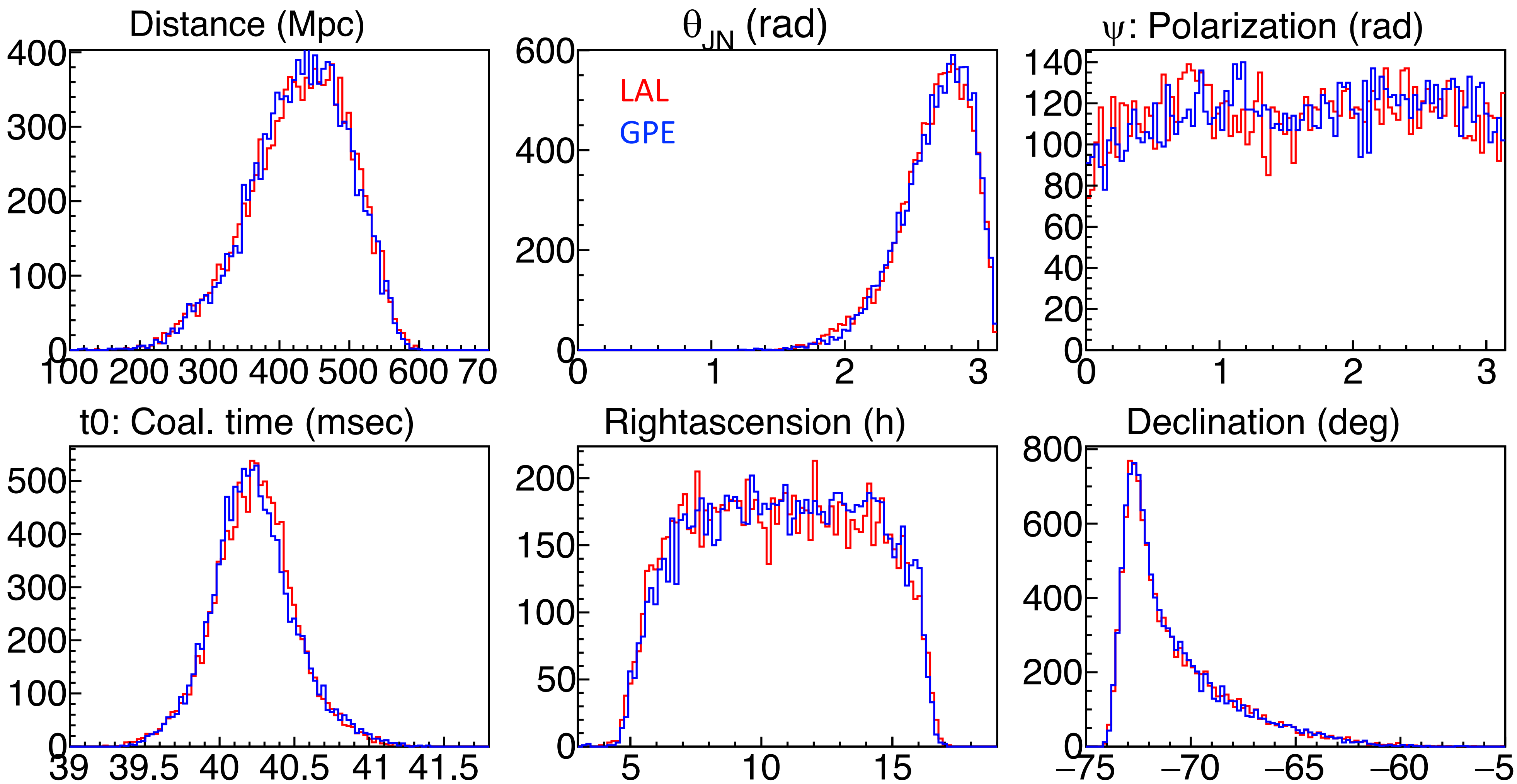

Comparisons (CBC parameter correlations)

Parameters in the final 500 live points (from 23 independent runs)

Note: they are not the posterior distributions

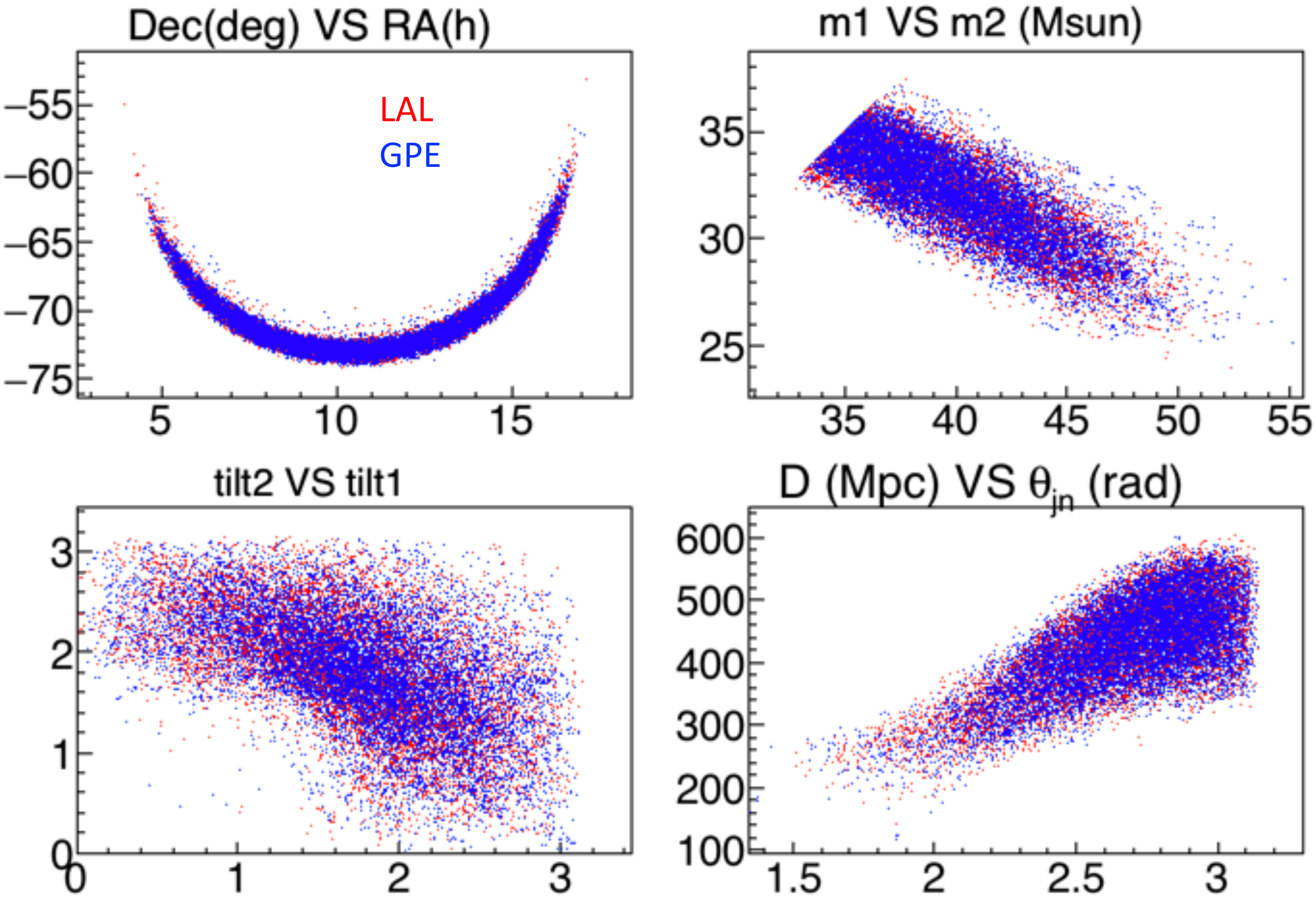

Outline

- G.P.E. – GPU accelerated Parameter Estimation
- Comparison of results – GW events analysis
- Comparison of results – Simulation
- Immediate future – O3 simulation
- Physics targets – O5 simulation

GW events analysis

- GW150914
  - Detailed studies done by LVC
    many official results have been published
- GW151226
  - Weaker but longer signal
- GW170814
  - Localization by LV
- GW170817
  - The first and (so far) the only BNS events

N_{live}= 2048, Time comsumption : 1~4 hours

GW150914 references

Referenced compared in this study

- PRL 116, 061102 : First detection
- PRL 116, 241102 : CBC parameter estimation
- PRD 93, 122004 : Minimal assumptions
- PRX 6, 041014 : Improved analysis
- PRX 6, 041015 : Review of O1 BH-BH events

PRX 6, 041014 – Improved analysis

- Full parameter (15) estimation with precessing-spin

	Precessing EOBNR	Precessing IMRPhenom	Overall
Detector-frame total mass $M/\mathrm{M}_\odot$	$71.6^{+4.3}_{-4.1}$	$70.9^{+4.0}_{-3.9}$	$71.3^{+4.3}_{-4.1}$
Detector-frame chirp mass $\mathcal{M}/\mathrm{M}_\odot$	$30.9^{+2.0}_{-1.9}$	$30.6^{+1.8}_{-1.8}$	$30.8^{+1.9}_{-1.8}$
Detector-frame primary mass $m_1/\mathrm{M}_\odot$	$38.9^{+5.1}_{-3.7}$	$38.5^{+5.6}_{-3.6}$	$38.7^{+5.3}_{-3.7}$
Detector-frame secondary mass $m_2/\mathrm{M}_\odot$	$32.7^{+3.6}_{-4.8}$	$32.2^{+3.6}_{-4.8}$	$32.5^{+3.7}_{-4.8}$
Detector-frame final mass $M_\mathrm{f}/\mathrm{M}_\odot$	$68.3^{+3.8}_{-3.7}$	$67.6^{+3.6}_{-3.5}$	$68.0^{+3.8}_{-3.6}$
Source-frame total mass $M^\mathrm{source}/\mathrm{M}_\odot$	$65.6^{+4.1}_{-3.8}$	$65.0^{+4.0}_{-3.6}$	$65.3^{+4.1}_{-3.7}$
Source-frame chirp mass $\mathcal{M}^\mathrm{source}/\mathrm{M}_\odot$	$28.3^{+1.8}_{-1.7}$	$28.1^{+1.7}_{-1.6}$	$28.2^{+1.8}_{-1.7}$
Source-frame primary mass $m_1^\mathrm{source}/\mathrm{M}_\odot$	$35.6^{+4.8}_{-3.4}$	$35.3^{+5.2}_{-3.4}$	$35.4^{+5.0}_{-3.4}$
Source-frame secondary mass $m_2^\mathrm{source}/\mathrm{M}_\odot$	$30.0^{+3.3}_{-4.4}$	$29.6^{+3.3}_{-4.3}$	$29.8^{+3.3}_{-4.3}$
Source-frame final mass $M_\mathrm{f}^\mathrm{source}/\mathrm{M}_\odot$	$62.5^{+3.7}_{-3.4}$	$62.0^{+3.7}_{-3.3}$	$62.2^{+3.7}_{-3.4}$
Mass ratio q	$0.84^{+0.14}_{-0.20}$	$0.84^{+0.14}_{-0.20}$	$0.84^{+0.14}_{-0.20}$
Effective inspiral spin parameter χ_eff	$-0.02^{+0.14}_{-0.16}$	$-0.05^{+0.13}_{-0.15}$	$-0.04^{+0.14}_{-0.16}$
Effective precession spin parameter χ_p	$0.28^{+0.38}_{-0.21}$	$0.35^{+0.45}_{-0.27}$	$0.31^{+0.44}_{-0.23}$
Dimensionless primary spin magnitude a_1	$0.22^{+0.43}_{-0.20}$	$0.32^{+0.53}_{-0.29}$	$0.26^{+0.52}_{-0.24}$
Dimensionless secondary spin magnitude a_2	$0.29^{+0.52}_{-0.27}$	$0.34^{+0.54}_{-0.31}$	$0.32^{+0.54}_{-0.29}$
Final spin a_f	$0.68^{+0.05}_{-0.05}$	$0.68^{+0.06}_{-0.06}$	$0.68^{+0.05}_{-0.06}$
Luminosity distance $D_\mathrm{L}/\mathrm{Mpc}$	440^{+160}_{-180}	440^{+150}_{-180}	440^{+160}_{-180}
Source redshift z	$0.094^{+0.032}_{-0.037}$	$0.093^{+0.029}_{-0.036}$	$0.093^{+0.030}_{-0.036}$
Upper bound on primary spin magnitude a_1	0.54	0.74	0.65
Upper bound on secondary spin magnitude a_2	0.70	0.78	0.75
Lower bound on mass ratio q	0.69	0.68	0.68

Comparison of results – GW150914

	PRX 6, 041014 (IMRPhenom)	GPE with LOSC data
SNR	23.7	23.7
Chirp mass (det.)	30.6 +1.8 -1.8	30.0 +2.2 -2.5
m1 (det.)	38.5 +5.6 -3.6	38.9 +5.9 -4.4
m2(det.)	32.2 +3.6 -4.8	31.1 +4.6 -6.7
Mass ratio	0.84 +0.14 -0.20	0.80 +0.13 -0.16
Chirp mass (source)	28.1 +1.7 -1.6	27.6 +1.9 -2.2
m1 (source)	35.3 +5.2 -3.4	35.7 +5.7 -3.9
m2 (source)	29.6 +3.3 -4.3	28.5 +4.1 -6.1
Luminosity distance (Mpc)	440 +160 -180	431 +150 -174
Source redshift	0.094 +0.032 -0.037	0.091 +0.035 -0.029
Effective inspiral spin χ_{eff}	-0.05 +0.13 -0.15	-0.03 +0.12 -0.14
Effective precession spin χ_p	0.35 +0.45 -0.27	0.32 +0.45 -0.25

PRD93, 122004 – Minimal assumptions

- Using burst analysis (not CBC) but sky localization errors are compared between with and without calibration errors (10%,10 deg)

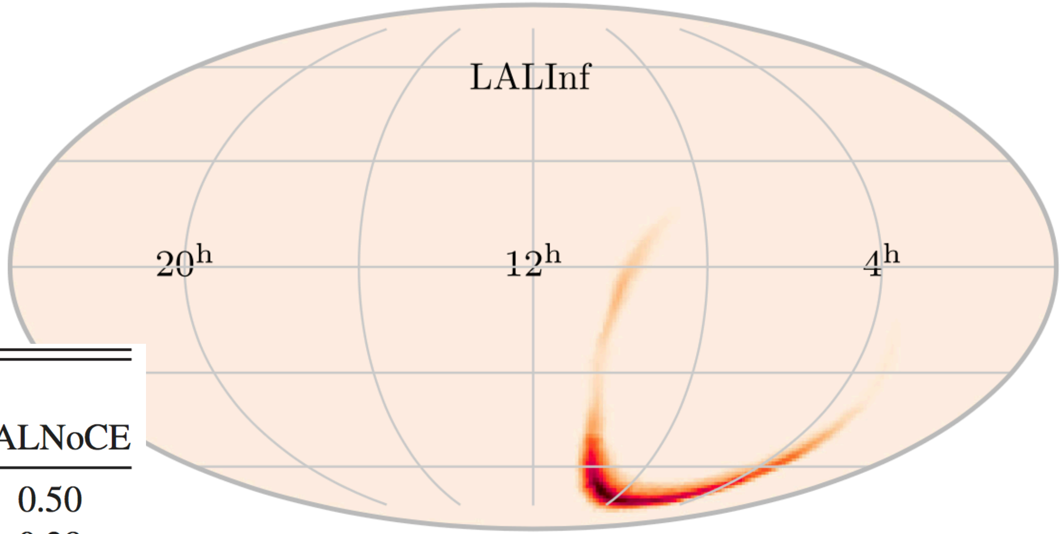

	Confidence regions 50%	Confidence regions 90%	Fidelity LIB	Fidelity BW	Fidelity LALInf	Fidelity LALNoCE
cWB	98 deg^2	308 deg^2	0.55	0.55	0.51	0.50
LIB	208 deg^2	746 deg^2	⋯	0.45	0.68	0.28
BW	101 deg^2	634 deg^2	⋯	⋯	0.68	0.87
LALInf	150 deg^2	610 deg^2	⋯	⋯	⋯	0.81
LALNoCE	48 deg^2	150 deg^2	⋯	⋯	⋯	⋯

PRX 6, 041015 – Review of O1 BBH events

- Using the improved calibration errors

	Amplitude		Phase	
Event	Hanford	Livingston	Hanford	Livingston
GW150914	4.8%	8.2%	3.2 deg	4.2 deg
LVT151012	4.2%	8.3%	2.7 deg	4.3 deg
GW151226	4.2%	6.9%	2.7 deg	3.6 deg

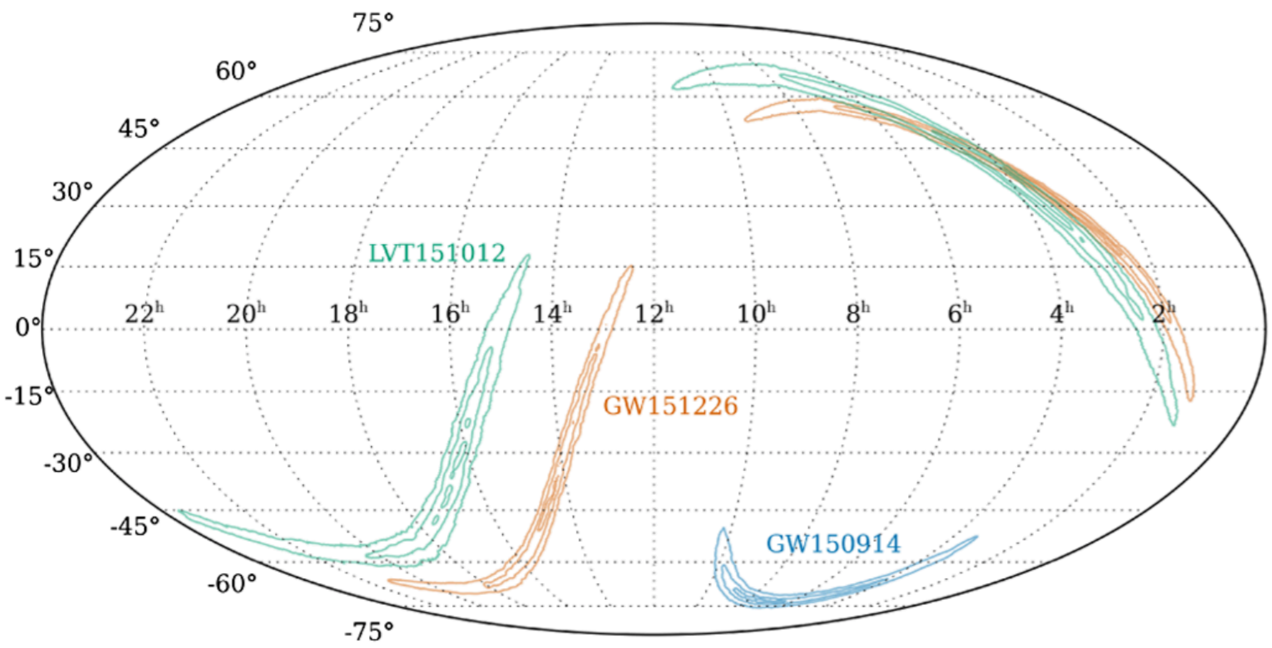

Comparison of results – GW150914

	PRD 6, 041014 (Burst)		GPE (LOSC data)	
	50 % C.L.	90 % C.L.	50 % C.L.	90 % C.L.
No C.E.	48 deg^2	150 deg^2	46 deg^2	158 deg^2
C.E. (5%, 5 deg)	—	—	78 deg^2	296 deg^2
C.E. (10%, 10 deg)	150 deg^2	610 deg^2	150 deg^2	577 deg^2
	PRX 6, 041015 (CBC)			
Improved C.E.	—	230 deg^2	67 deg^2	236 deg^2

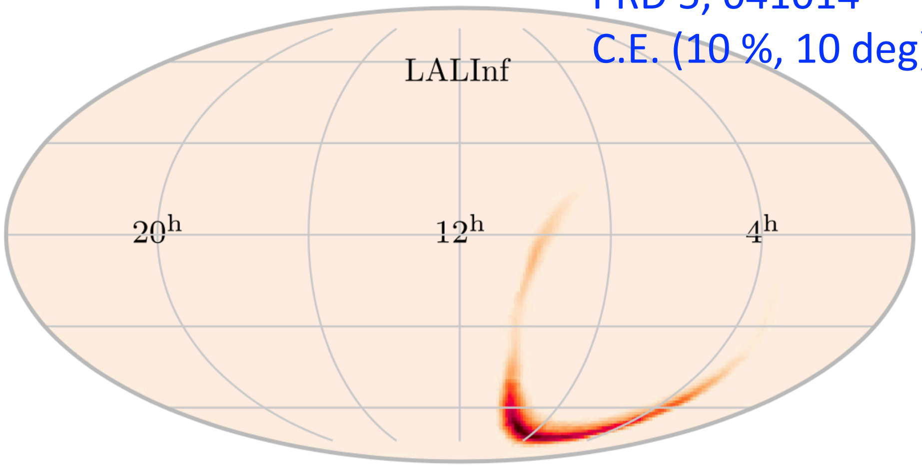

PRD 5, 041014
C.E. (10 %, 10 deg)

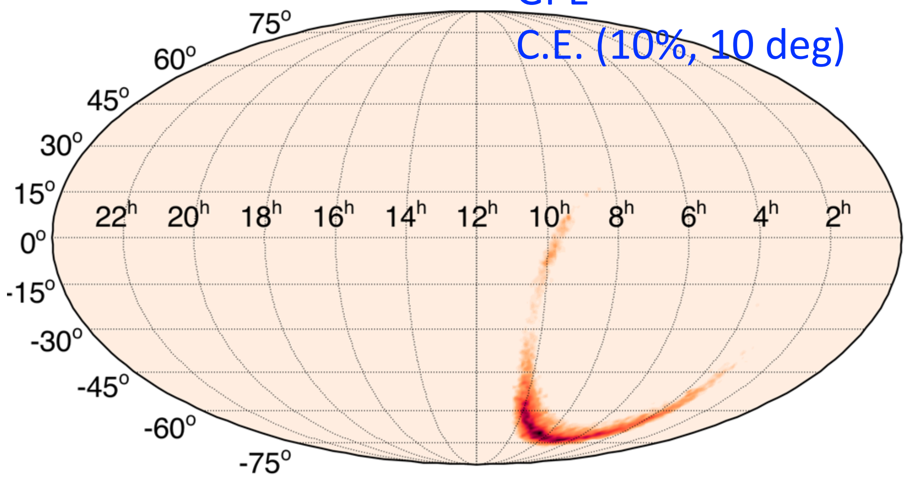

GPE
C.E. (10%, 10 deg)

GW151226 references

References compared in this study

- PRL 116, 241103
- PRX 6, 041015

Primary black hole mass	$14.2^{+8.3}_{-3.7} M_\odot$
Secondary black hole mass	$7.5^{+2.3}_{-2.3} M_\odot$
Chirp mass	$8.9^{+0.3}_{-0.3} M_\odot$
Total black hole mass	$21.8^{+5.9}_{-1.7} M_\odot$
Final black hole mass	$20.8^{+6.1}_{-1.7} M_\odot$
Radiated gravitational-wave energy	$1.0^{+0.1}_{-0.2} M_\odot c^2$
Peak luminosity	$3.3^{+0.8}_{-1.6} \times 10^{56}$ erg/s
Final black hole spin	$0.74^{+0.06}_{-0.06}$
Luminosity distance	440^{+180}_{-190} Mpc
Source redshift z	$0.09^{+0.03}_{-0.04}$

	GW151226 EOBNR	IMRPhenom	Overall
Detector frame			
Total mass $M/\mathrm{M}_\odot$	$23.6^{+8.0}_{-1.3}$	$23.8^{+5.1}_{-1.5}$	$23.7^{+6.5\pm2.2}_{-1.4\pm0.1}$
Chirp mass $\mathcal{M}/\mathrm{M}_\odot$	$9.71^{+0.08}_{-0.07}$	$9.72^{+0.06}_{-0.06}$	$9.72^{+0.07\pm0.01}_{-0.06\pm0.01}$
Primary mass $m_1/\mathrm{M}_\odot$	$15.3^{+10.8}_{-3.8}$	$15.8^{+7.2}_{-4.0}$	$15.6^{+9.0\pm2.6}_{-4.0\pm0.2}$
Secondary mass $m_2/\mathrm{M}_\odot$	$8.3^{+2.5}_{-2.9}$	$8.1^{+2.5}_{-2.1}$	$8.2^{+2.6\pm0.2}_{-2.5\pm0.5}$
Final mass $M_\mathrm{f}/\mathrm{M}_\odot$	$22.5^{+8.2}_{-1.4}$	$22.8^{+5.3}_{-1.6}$	$22.6^{+6.7\pm2.2}_{-1.5\pm0.1}$
Source frame			
Total mass $M^\mathrm{source}/\mathrm{M}_\odot$	$21.6^{+7.4}_{-1.6}$	$21.9^{+4.7}_{-1.7}$	$21.8^{+5.9\pm2.0}_{-1.7\pm0.1}$
Chirp mass $\mathcal{M}^\mathrm{source}/\mathrm{M}_\odot$	$8.87^{+0.35}_{-0.28}$	$8.90^{+0.31}_{-0.27}$	$8.88^{+0.33\pm0.01}_{-0.28\pm0.04}$
Primary mass $m_1^\mathrm{source}/\mathrm{M}_\odot$	$14.0^{+10.0}_{-3.5}$	$14.5^{+6.6}_{-3.7}$	$14.2^{+8.3\pm2.4}_{-3.7\pm0.2}$
Secondary mass $m_2^\mathrm{source}/\mathrm{M}_\odot$	$7.5^{+2.3}_{-2.6}$	$7.4^{+2.3}_{-2.0}$	$7.5^{+2.3\pm0.2}_{-2.3\pm0.4}$
Final mass $M_\mathrm{f}^\mathrm{source}/\mathrm{M}_\odot$	$20.6^{+7.6}_{-1.6}$	$20.9^{+4.8}_{-1.8}$	$20.8^{+6.1\pm2.0}_{-1.7\pm0.1}$
Energy radiated $E_\mathrm{rad}/(\mathrm{M}_\odot c^2)$	$1.02^{+0.09}_{-0.24}$	$0.99^{+0.11}_{-0.17}$	$1.00^{+0.10\pm0.01}_{-0.20\pm0.03}$
Mass ratio q	$0.54^{+0.40}_{-0.33}$	$0.51^{+0.39}_{-0.25}$	$0.52^{+0.40\pm0.03}_{-0.29\pm0.04}$
Effective inspiral spin χ_eff	$0.21^{+0.24}_{-0.11}$	$0.22^{+0.15}_{-0.08}$	$0.21^{+0.20\pm0.07}_{-0.10\pm0.03}$
Primary spin magnitude a_1	$0.42^{+0.35}_{-0.37}$	$0.55^{+0.35}_{-0.42}$	$0.49^{+0.37\pm0.11}_{-0.42\pm0.07}$
Secondary spin magnitude a_2	$0.51^{+0.44}_{-0.46}$	$0.52^{+0.42}_{-0.47}$	$0.52^{+0.43\pm0.01}_{-0.47\pm0.00}$
Final spin a_f	$0.73^{+0.05}_{-0.06}$	$0.75^{+0.07}_{-0.05}$	$0.74^{+0.06\pm0.03}_{-0.06\pm0.03}$
Luminosity distance $D_\mathrm{L}/\mathrm{Mpc}$	450^{+180}_{-210}	440^{+170}_{-180}	$440^{+180\pm20}_{-190\pm10}$
Source redshift z	$0.096^{+0.035}_{-0.042}$	$0.092^{+0.033}_{-0.037}$	$0.094^{+0.035\pm0.004}_{-0.039\pm0.001}$
Upper bound			
Primary spin magnitude a_1	0.68	0.83	0.77 ± 0.12
Secondary spin magnitude a_2	0.90	0.89	0.90 ± 0.01
Lower bound			
Mass ratio q	0.25	0.30	0.28 ± 0.04
Log Bayes factor $\ln \mathcal{B}_{s/n}$	59.5 ± 0.1	60.2 ± 0.2	⋯
Information criterion DIC	34296.4 ± 0.2	34295.1 ± 0.1	⋯

Comparison of results – GW151226

	PRX 6, 041015 (IMRPhenom)	GPE with LOSC data
SNR	13.0	12.1
Chirp mass (source)	8.90 +0.31 -0.27	8.92 +0.37 -0.33
m1 (source)	14.5 +6.6 -3.7	14.0 +6.2 -3.4
m2 (source)	7.4 +2.3 -2.0	7.7 +2.2 -2.0
Luminosity distance (Mpc)	440 +170 -180	441 +196 -195
Source redshift	0.092 +0.033 -0.037	0.095 +0.039 -0.037
Effective inspiral spin χeff	0.22 +0.15 -0.08	0.23 +0.14 -0.11
Primary spin magnitude a_1	0.55 +0.35 -0.42	0.56 +0.35 -0.44
Primary spin magnitude a_2	0.52 +0.42 -0.47	0.56 +0.39 -0.50

SNR could not be reproduced exactly as in the publication
Maybe we need additional cleaning of LOSC public data

Comparison of results – GW151226

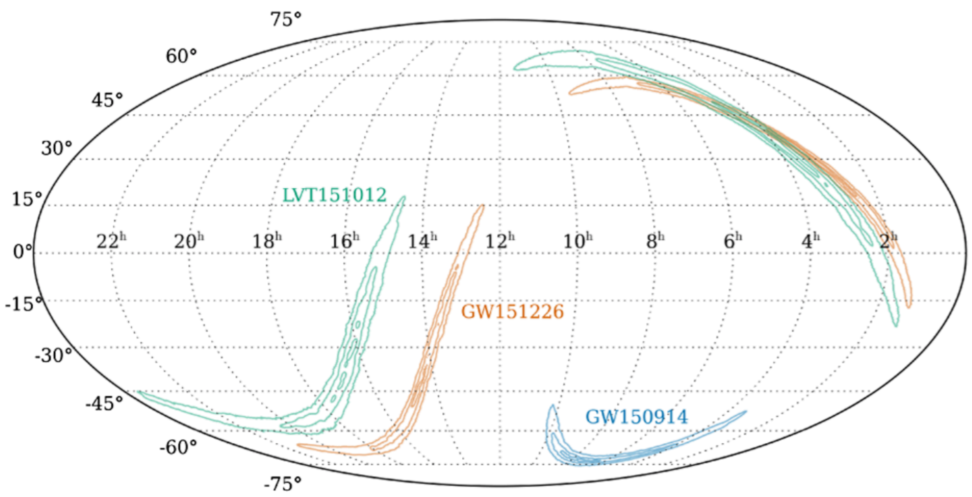

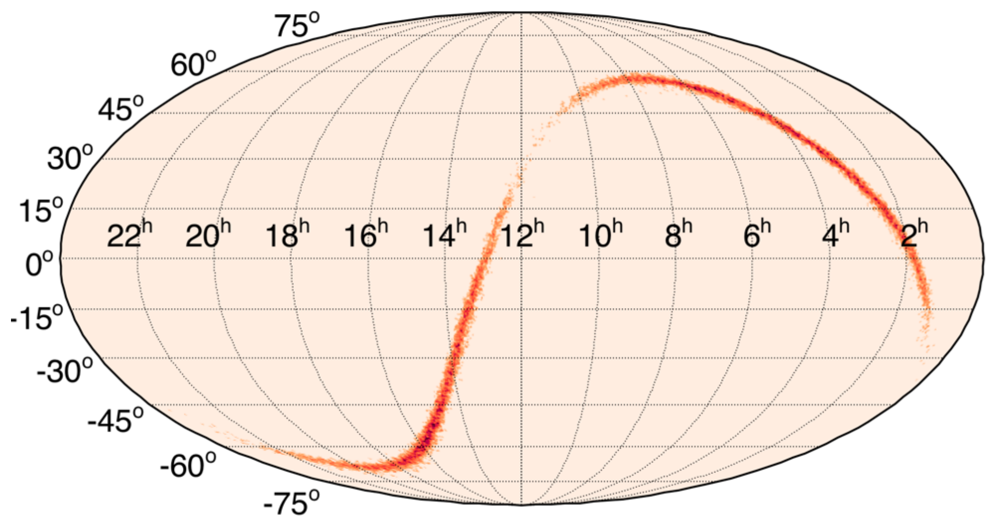

GW151226: (PRX 6, 041015)
90 % ΔΩ = 850 deg2

GPE
90 % ΔΩ = 863 deg2

GW170814 reference

References compared in this study

- PRL 119, 141101

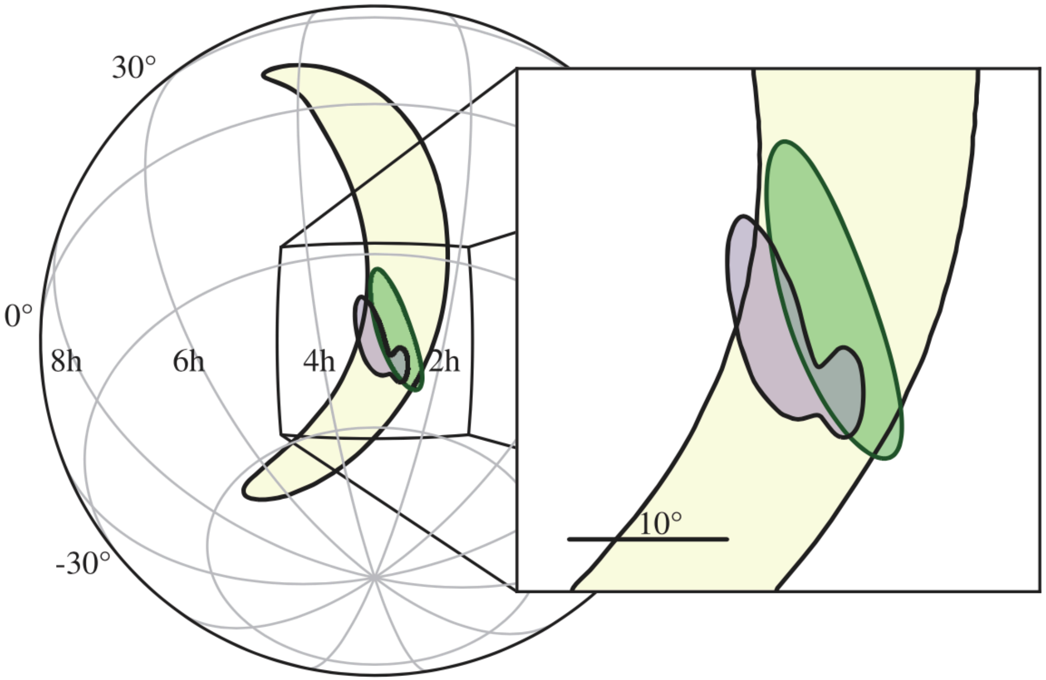

Primary black hole mass m_1	$30.5^{+5.7}_{-3.0} M_\odot$
Secondary black hole mass m_2	$25.3^{+2.8}_{-4.2} M_\odot$
Chirp mass $\mathcal{M}$	$24.1^{+1.4}_{-1.1} M_\odot$
Total mass M	$55.9^{+3.4}_{-2.7} M_\odot$
Final black hole mass M_f	$53.2^{+3.2}_{-2.5} M_\odot$
Radiated energy $E_{\rm rad}$	$2.7^{+0.4}_{-0.3} M_\odot\ c^2$
Peak luminosity $\ell_{\rm peak}$	$3.7^{+0.5}_{-0.5} \times 10^{56}$ erg s^{-1}
Effective inspiral spin parameter $\chi_{\rm eff}$	$0.06^{+0.12}_{-0.12}$
Final black hole spin a_f	$0.70^{+0.07}_{-0.05}$
Luminosity distance D_L	540^{+130}_{-210} Mpc
Source redshift z	$0.11^{+0.03}_{-0.04}$

Comparison of results – GW170814

	PRX 6, 041015 (IMRPhenom)	GPE with LOSC data (CLN)
SNR	16.1	16.6
SNR (H,L,V)	7.3, 13.7, 4.4	9.5, 13.1, 4.0
Chirp mass (source)	24.1 +1.4 -1.1	23.2 +2.0 -2.1
m1 (source)	30.5 +5.7 -3.0	30.7 +6.9 -4.1
m2 (source)	25.3 +2.8 -4.2	23.2 +4.1 -5.0
Luminosity distance (Mpc)	540 +130 -210	462 +157 -168
Source redshift	0.11 +0.03 -0.04	0.10 +0.03 -0.03
Effective inspiral spin χ_{eff}	0.06 +0.12 -0.12	-0.06 +0.18 -0.21

Comparison of results – GW170814

LIGO-T1700453

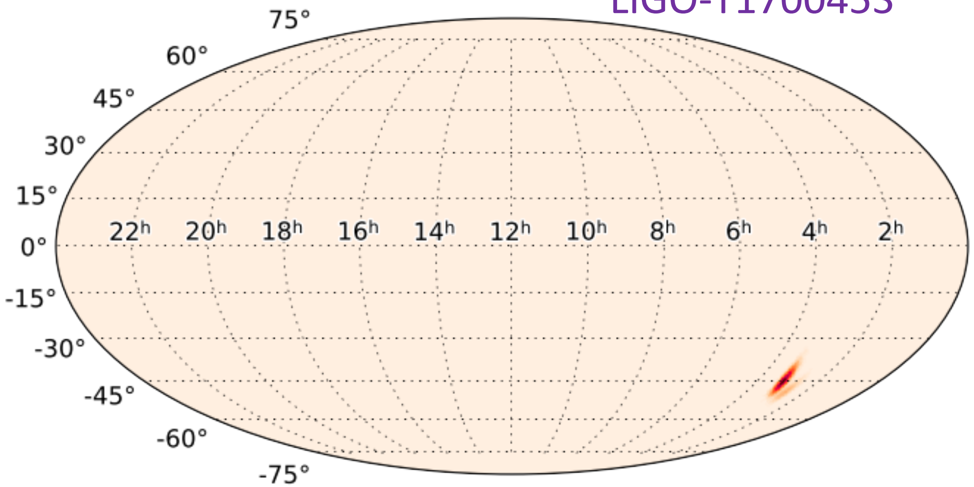

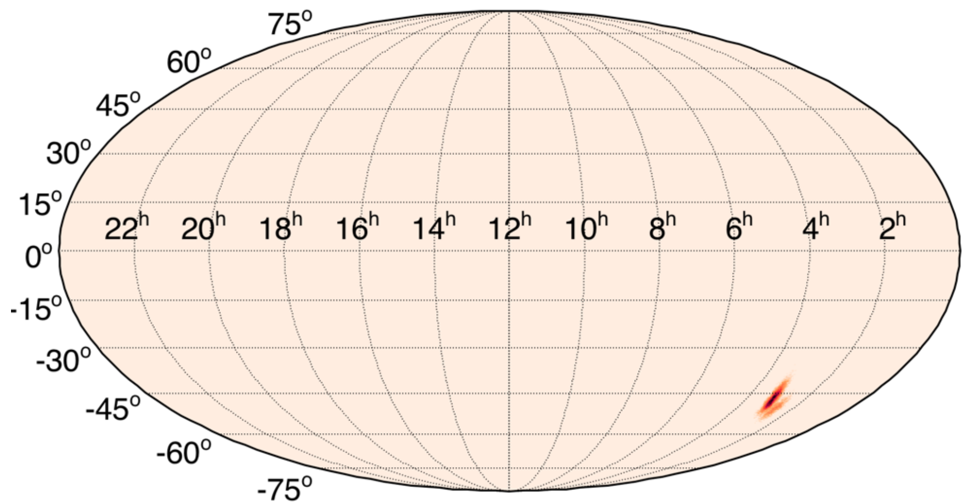

PRL 119. 141101
90 % ΔΩ = 60 deg2

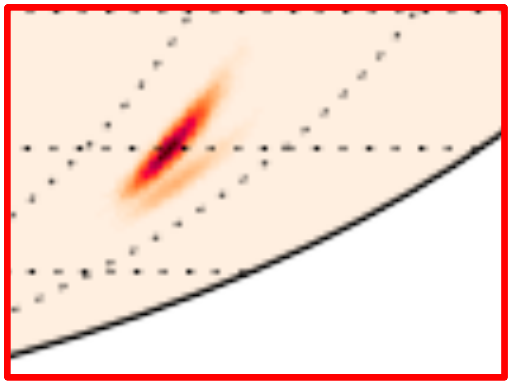

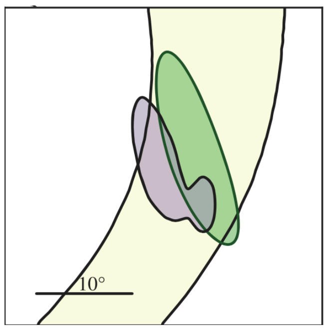

GPE
90 % ΔΩ = 55 deg2

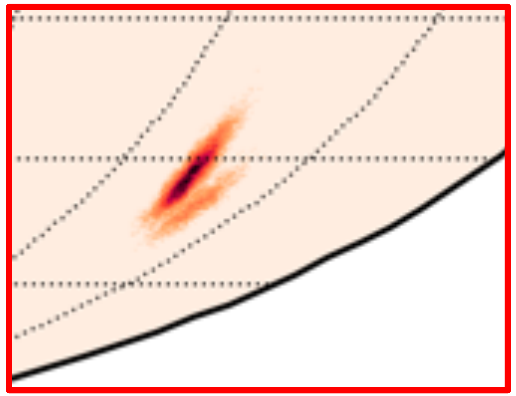

GW170817 reference

References compared in this study

- PRL 119, 161101

	Low-spin priors ($\lvert\chi\rvert \le 0.05$)	High-spin priors ($\lvert\chi\rvert \le 0.89$)
Primary mass m_1	1.36–1.60 $M_\odot$	1.36–2.26 $M_\odot$
Secondary mass m_2	1.17–1.36 $M_\odot$	0.86–1.36 $M_\odot$
Chirp mass $\mathcal{M}$	$1.188^{+0.004}_{-0.002} M_\odot$	$1.188^{+0.004}_{-0.002} M_\odot$
Mass ratio m_2/m_1	0.7–1.0	0.4–1.0
Total mass $m_{\rm tot}$	$2.74^{+0.04}_{-0.01} M_\odot$	$2.82^{+0.47}_{-0.09} M_\odot$
Radiated energy $E_{\rm rad}$	$> 0.025 M_\odot c^2$	$> 0.025 M_\odot c^2$
Luminosity distance $D_{\rm L}$	40^{+8}_{-14} Mpc	40^{+8}_{-14} Mpc
Viewing angle Θ	$\le 55°$	$\le 56°$
Using NGC 4993 location	$\le 28°$	$\le 28°$
Combined dimensionless tidal deformability $\tilde{\Lambda}$	≤ 800	≤ 700
Dimensionless tidal deformability $\Lambda(1.4 M_\odot)$	≤ 800	≤ 1400

Comparison of results – GW170817

Low spin priors ($|\chi| < 0.05$)

	PRX 6, 041015 (IMRPhenom)	GPE with LOSC data (CLN)
SNR	32.4	37.2
SNR (H,L,V)	18.8, 26.4, 2.0	21.9, 29.8, 3.8
Chirp mass (source)	1.188 +0.004 -0.002	1.188 +0.005 -0.003
m1 (source)	1.36 – 1.60	1.36 – 1.72
m2 (source)	1.17 – 1.36	1.09 – 1.36
Mass ratio	0.7 – 1.0	0.63 – 0.98
Distance	40 +8 -14	36 +10 -20

Comparison of results – GW170817

High spin priors ($|\chi| < 0.89$)

	PRX 6, 041015 (IMRPhenom)	GPE with LOSC data (CLN)
SNR	32.4	37.2
SNR (H,L,V)	18.8, 26.4, 2.0	21.9, 29.8, 3.7
Chirp mass (source)	1.188 +0.004 -0.002	1.188 +0.005 -0.003
m1 (source)	1.36 – 2.26	1.36 – 2.12
m2 (source)	0.86 – 1.36	0.91 – 1.36
Mass ratio	0.4 – 1.0	0.43 – 0.97
Distance	40 +8 -14	36 +11 -20

Comparison of results – GW170817

LIGO-G1701985

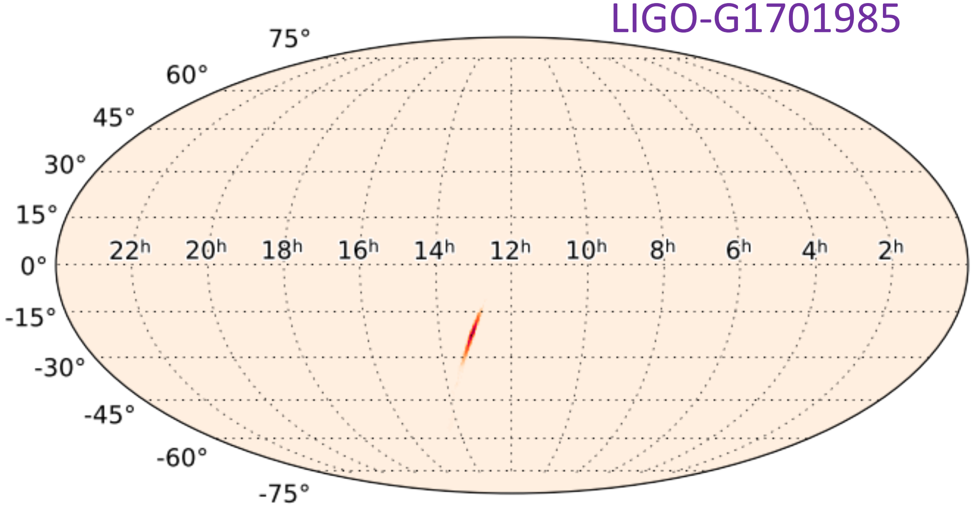

PRL 119. 141101
90 % ΔΩ = 28 deg2

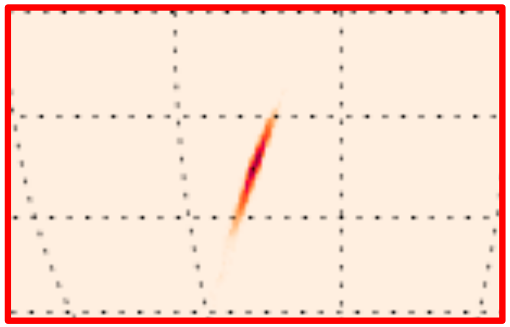

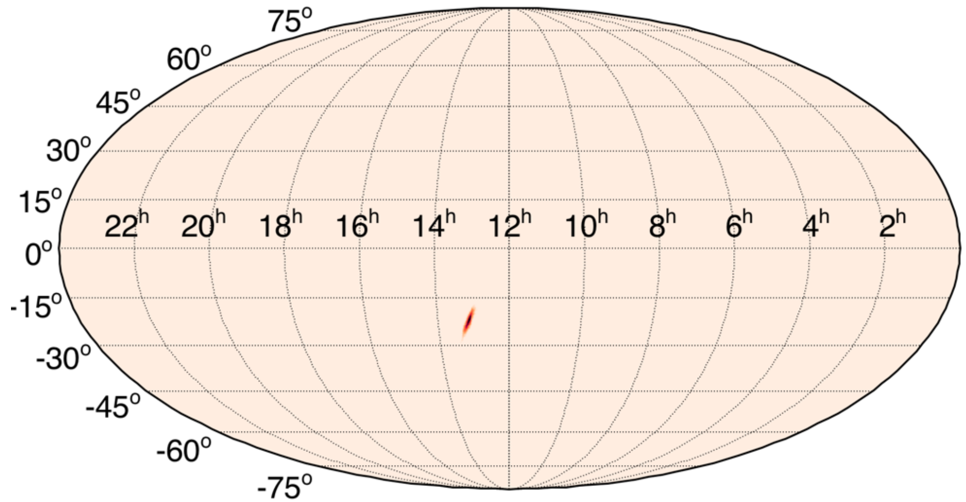

GPE ($|\chi| < 0.05$)
90 % ΔΩ = 13.5 deg2

GPE ($|\chi| < 0.89$)
90 % ΔΩ = 14.3 deg2

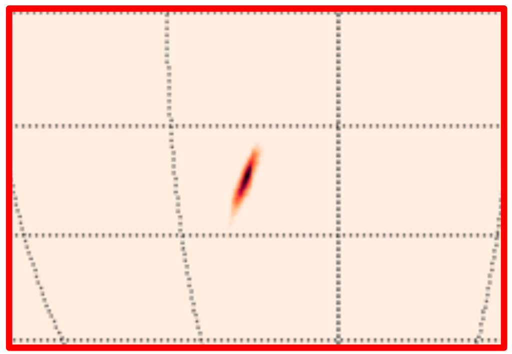

Outline

- G.P.E. – GPU accelerated Parameter Estimation
- Comparison of results – GW events analysis
- Comparison of results – Simulation
- Immediate future – O3 simulation
- Physics targets – O5 simulation

Comparison (KAGRA 40 Mpc)

Based on Narikawa-san's list: TF2_15BNS125_40Mpc_i30deg.xml

Event #	SNR(H)		SNR(L)		SNR(V)		SNR(K)		Network	
	TN	SH	TN	SH	TN	SH	TN	SH	TN	SH
10	42.2	42.2	43.2	43.2	9.2	9.2	7.8	7.8	61.6	61.6

Ev. #	$\Delta\Omega$ (HL)		$\Delta\Omega$ (HLV)		$\Delta\Omega$ (HLK)		$\Delta\Omega$ (HVK)		$\Delta\Omega$ (LVK)		$\Delta\Omega$(HLVK)	
	TN	SH	TN	SH	TN	SH	TN	SH	TN	SH	TN	SH
10	167	144	5.5	5.9	25.5	27.1	8.1	9.3	6.9	6.6	5.3	5.6

Agreements between TN and SH results

Comparison

Event #10 <HL> $\Delta\Omega$ = 167 (TN), 144 (SH) deg^2

TN

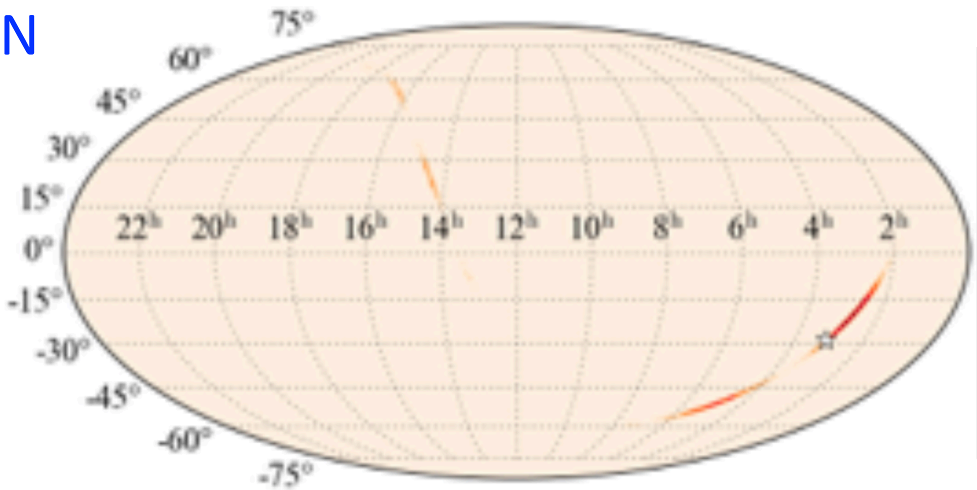

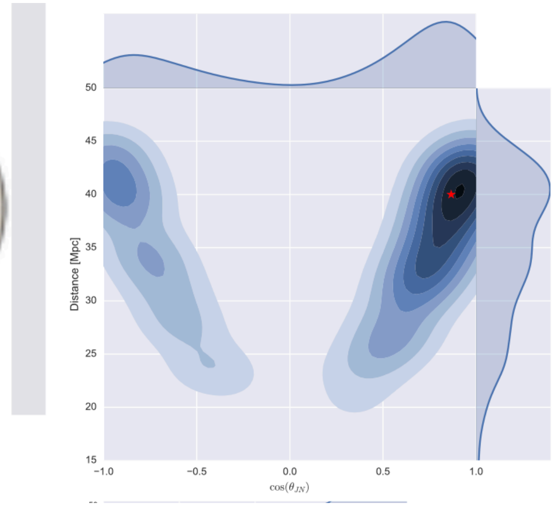

SH

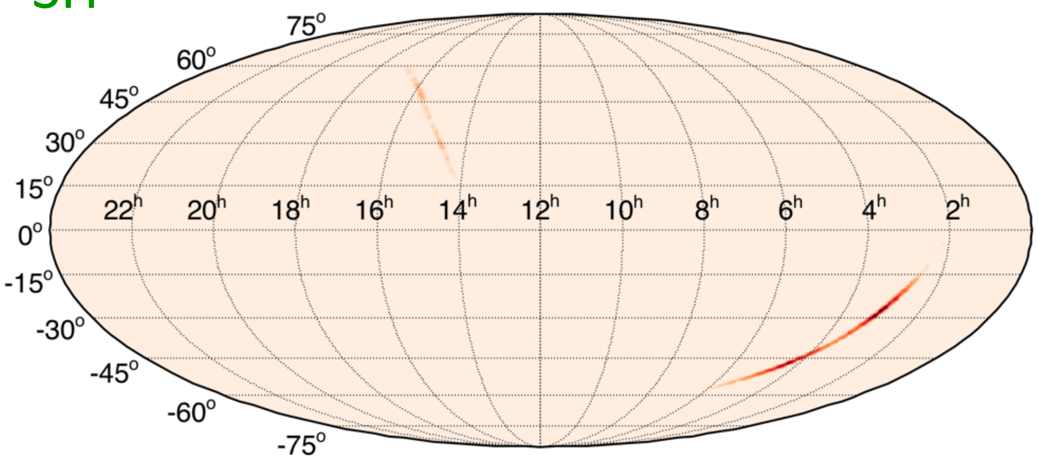

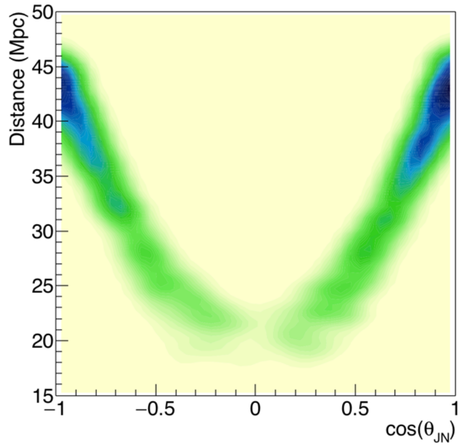

Injected signal SNR

Based on Narikawa-san's list: TF2_15BNS125_40Mpc_i30deg.xml

Event #	SNR(H)		SNR(L)		SNR(V)		SNR(K)		Network	
	TN	SH	TN	SH	TN	SH	TN	SH	TN	SH
2	19.4	19.4	26.2	26.2	2.7	2.7	3.5	3.5	32.9	32.9
271	25.2	25.2	8.8	8.8	12.4	12.4	3.4	3.4	29.7	29.7
287	16.3	16.3	18.1	18.1	7.5	7.5	3.6	3.6	25.7	25.7
294	27.5	27.4	15.4	15.4	12.0	12.0	3.5	3.5	33.9	33.9
300	20.1	20.1	12.9	12.9	10.7	10.7	3.6	3.6	26.4	26.4
306	18.1	18.1	16.8	16.8	8.8	8.8	3.7	3.7	26.5	26.4
320	21.9	21.9	17.0	17.0	10.2	10.2	3.7	3.7	29.8	29.8

Comparison

Wide Prior

comp-min	comp-max	Mc-min	Mc-max	q-min	flow	fhigh	srate	seglen	seed	Nlive
0.6	5.0	1.13	1.40244	0.125	23	2048	4096	128	1234	2048

test run

/home/handai/narikawa/MCMC/Toward_03/BNS/event2
TF2_15BNS125_40Mpc_i30deg.xml

Event #	2	271	287	294	300	306	320
ΔΩ TN	22.29	11.06	17.15	7.92	12.48	11.75	11.22
ΔΩ SH	25.98	10.42	11.18	9.88	11.7	11.68	10.73

Outline

- G.P.E. – GPU accelerated Parameter Estimation
- Comparison of results – GW events analysis
- Comparison of results – Simulation
- Immediate future – O3 simulation
- Physics targets – O5 simulation

O3 simulation

- LIGO 116 Mpc
- Virgo 62.9 Mpc
- KAGRA 9.5 Mpc

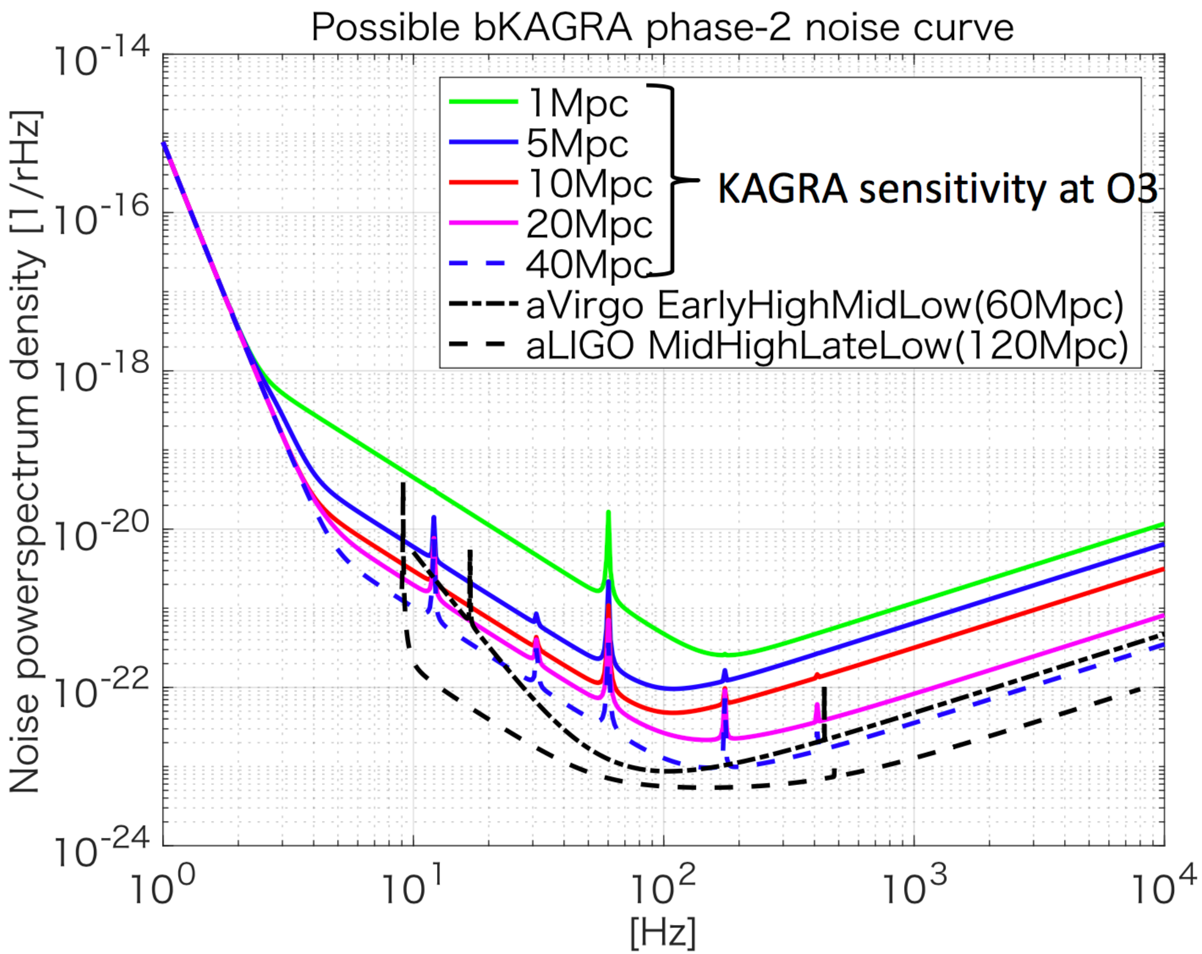

KAGRA's sensitivity curves: by Enomoto, Michimura
LIGO, Virgo: taken from arXiv:1304.0670

Detector antenna patterns

Sqrt($F_p^2+F_x^2$)

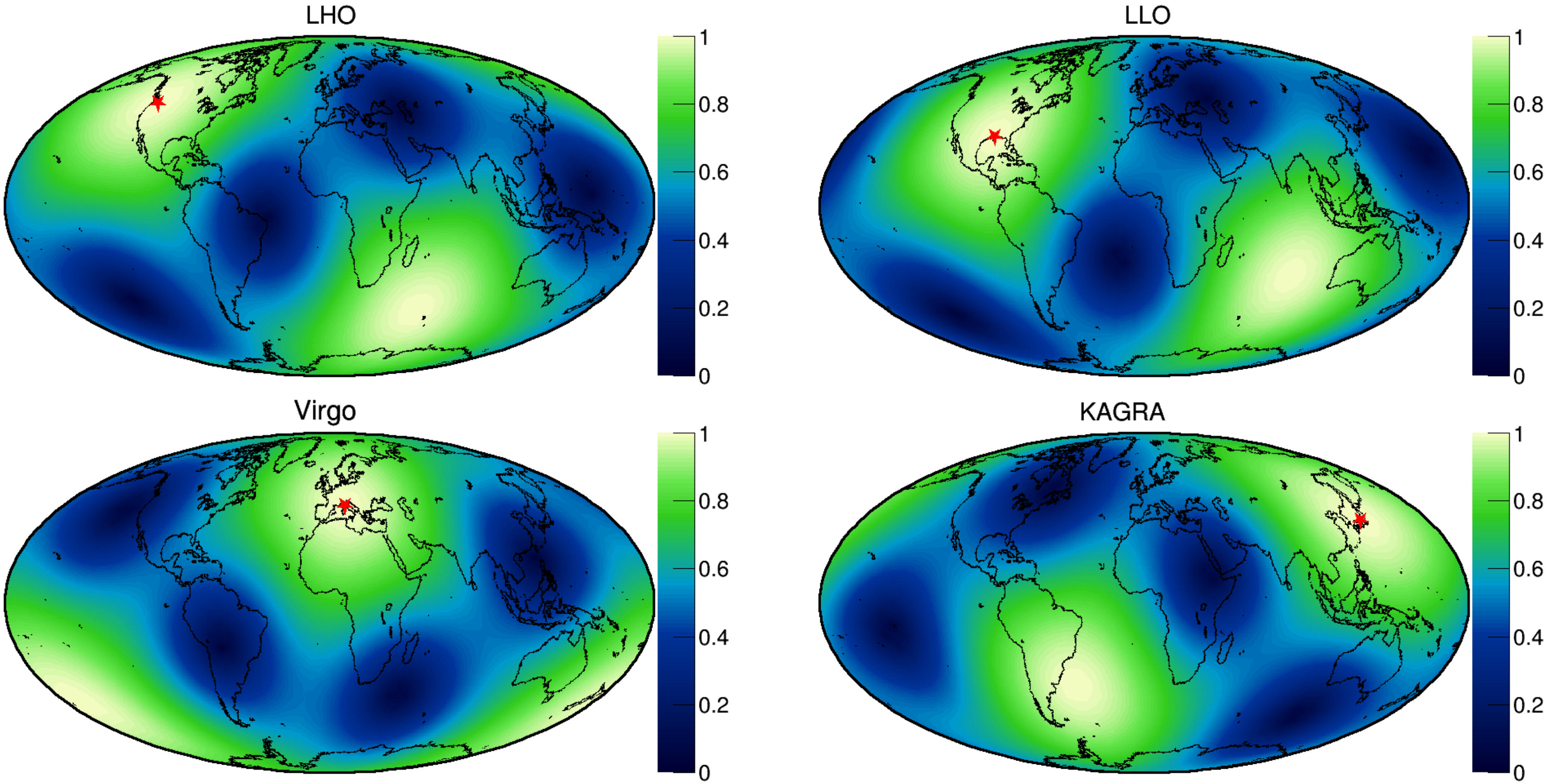

O3 simulation

Fix distance of BNS at 40 Mpc, then …

- Randomly distribute (BNS: 1.4-1.4)
  - inclination
  - polarization
  - sky location

  (25,000 = 5,000 events x5 detector cases)

- Fix: inclination (4) (BNS: 1.5-1.25)
  and polarization (5)
  - Uniformly distribute source location (192)

  (15,360 = 192 x5 x4 x4 sensitivity cases)

Condition1 : Random inclination

Tagoshi-san's results

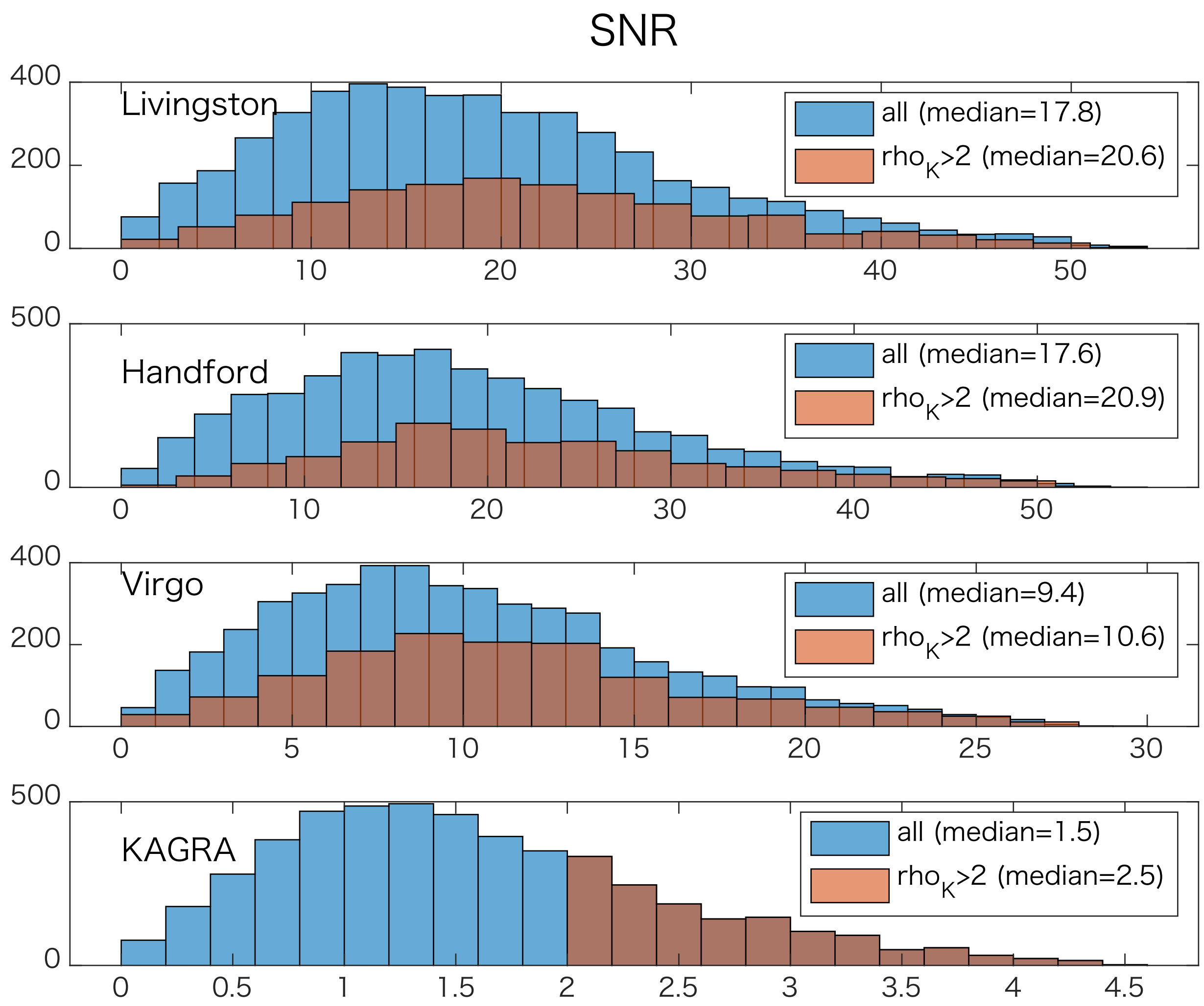

Condition1 : Random inclination

Tagoshi-san's results

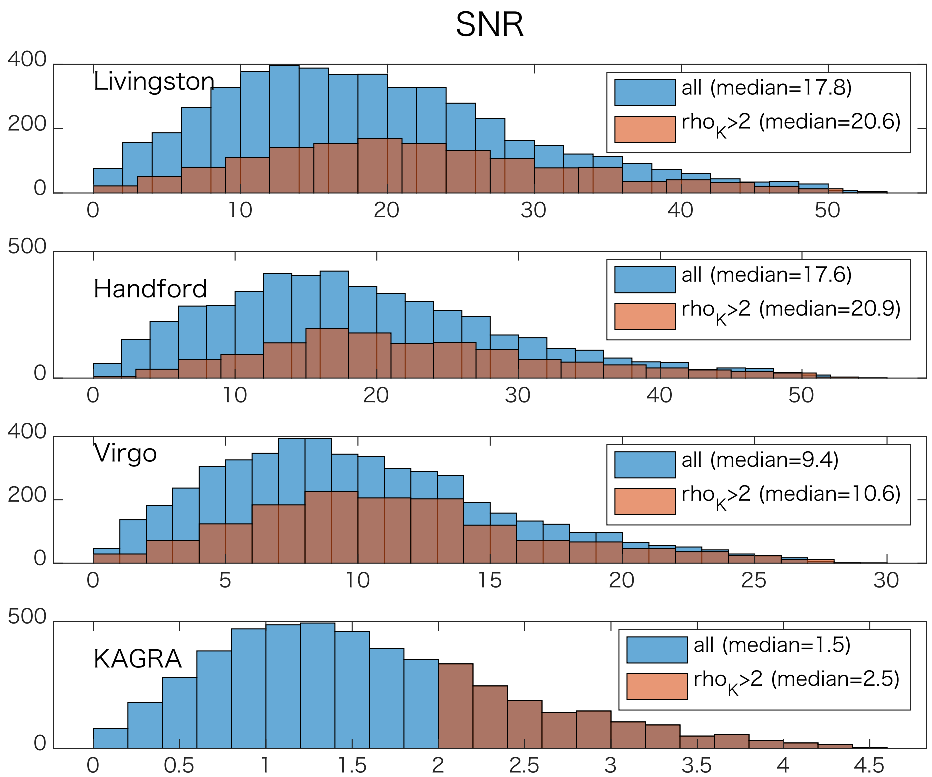

SH

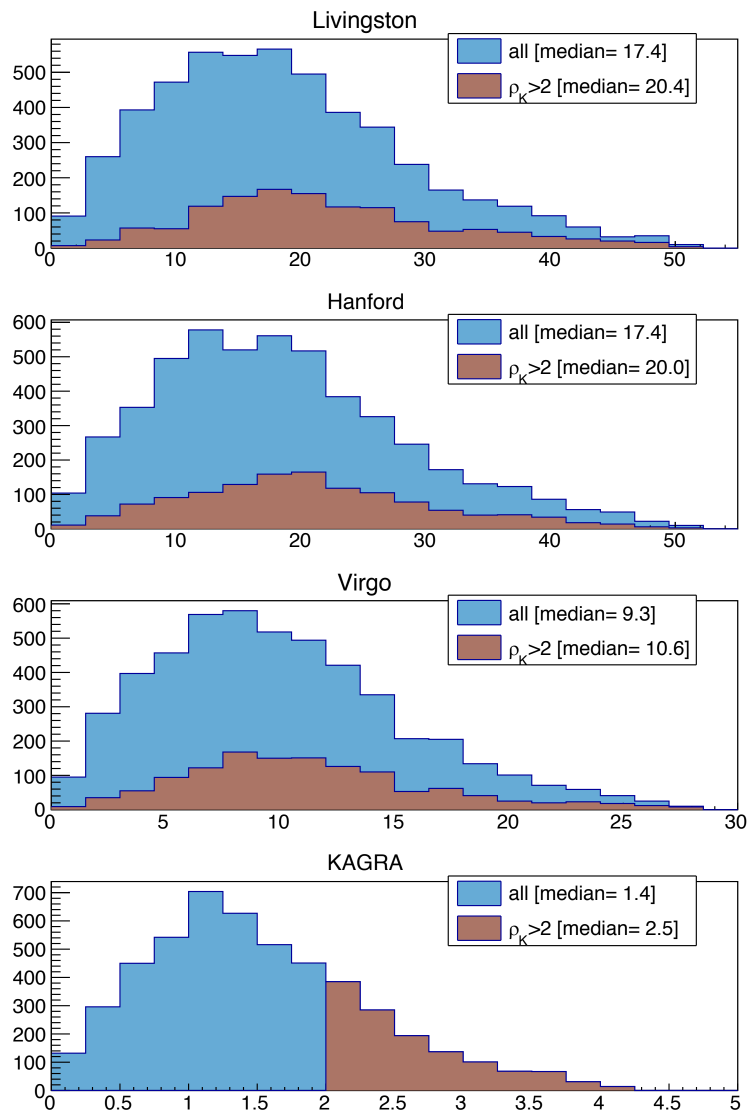

Condition1 : Random inclination

Tagoshi-san's results

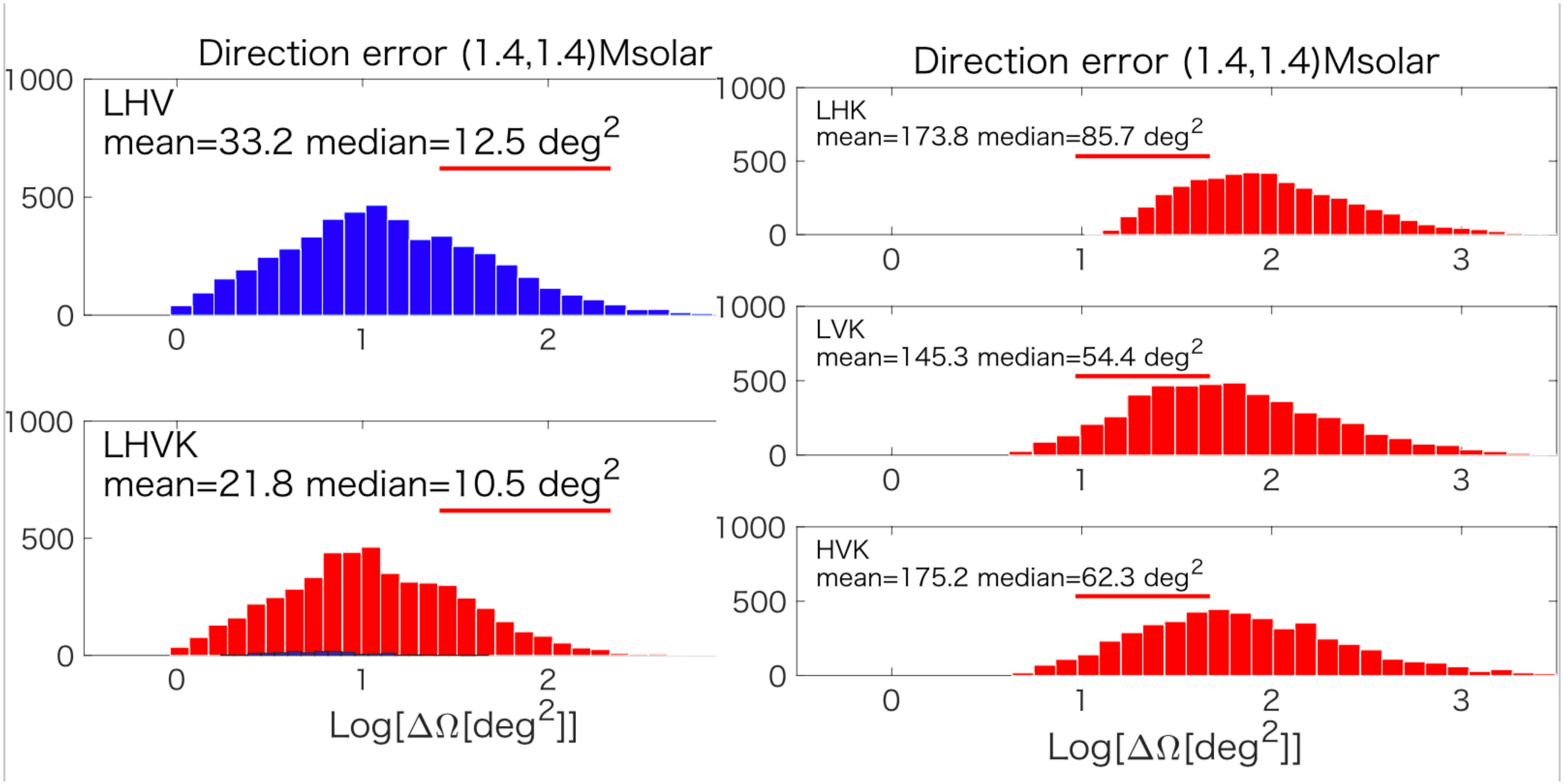

Condition1 : Random inclination

Tagoshi-san's results

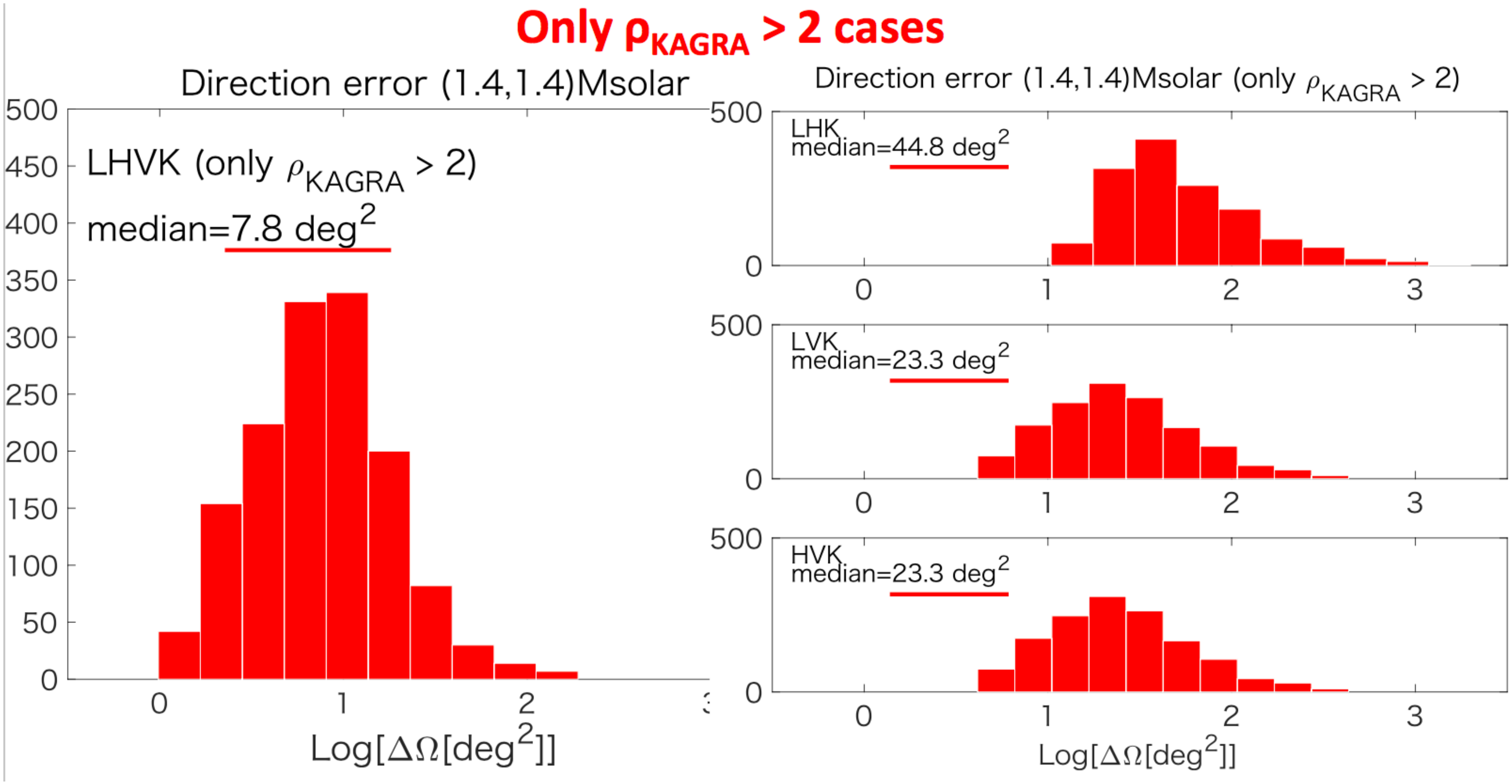

Condition1 : Random inclination

SH

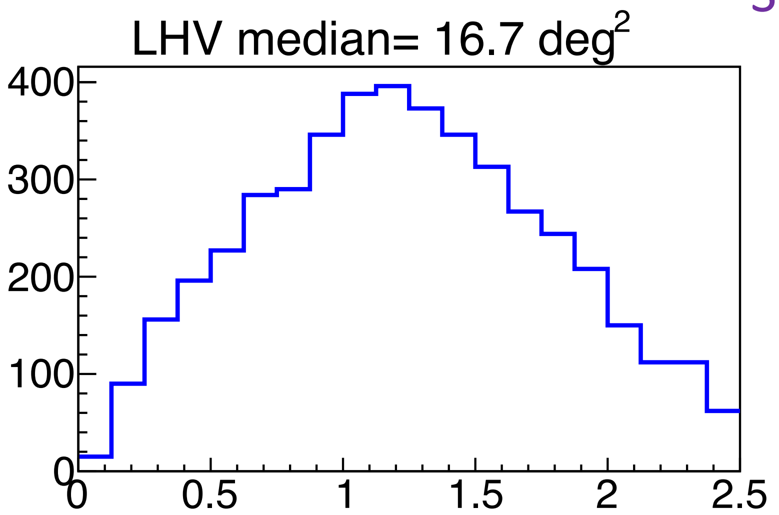

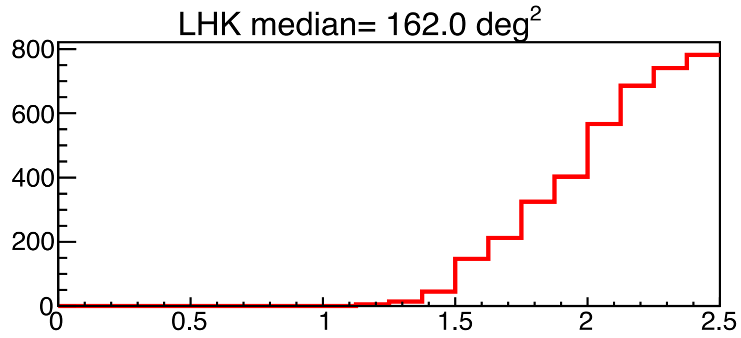

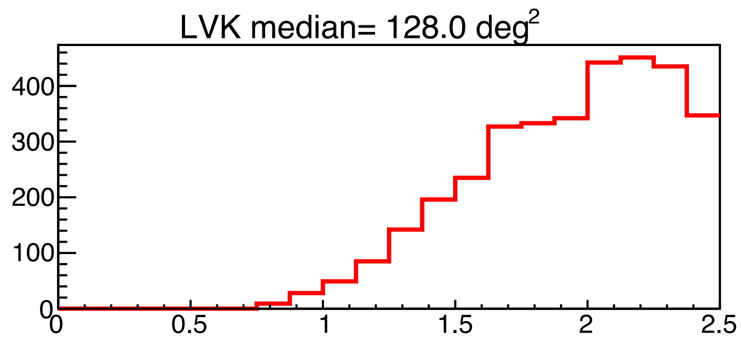

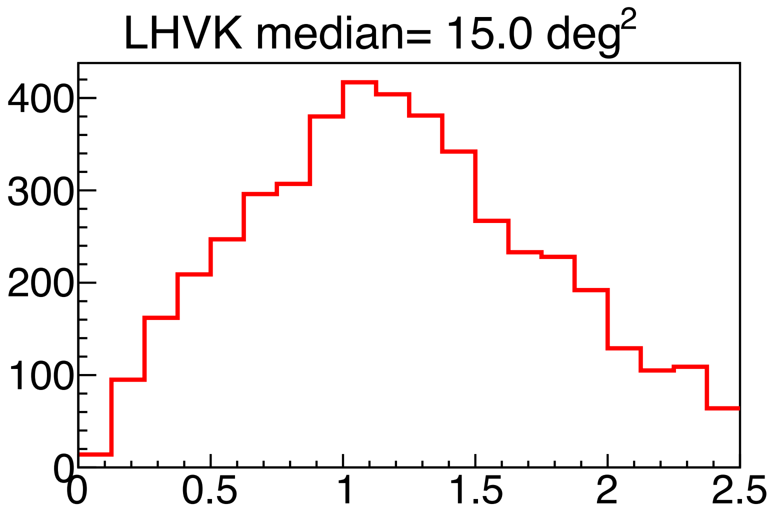

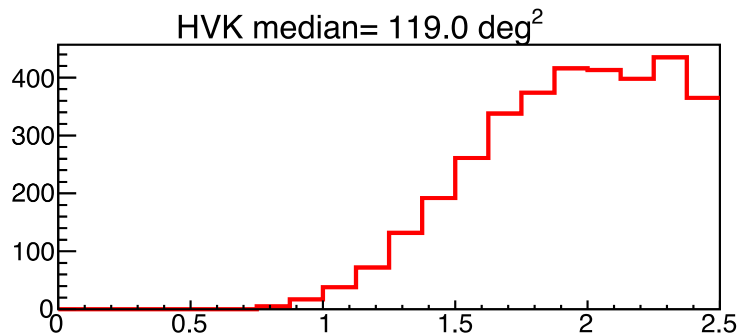

Condition1 : Random inclination

Tagoshi-san's results

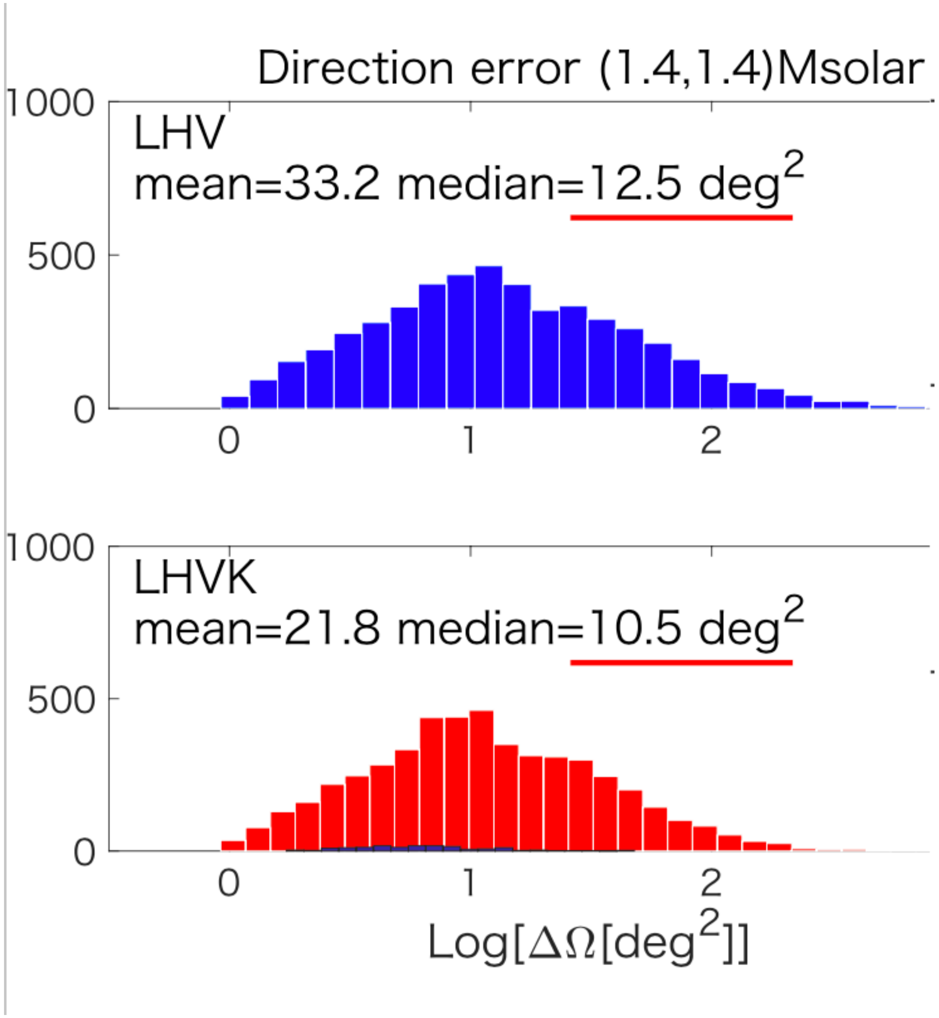

SH

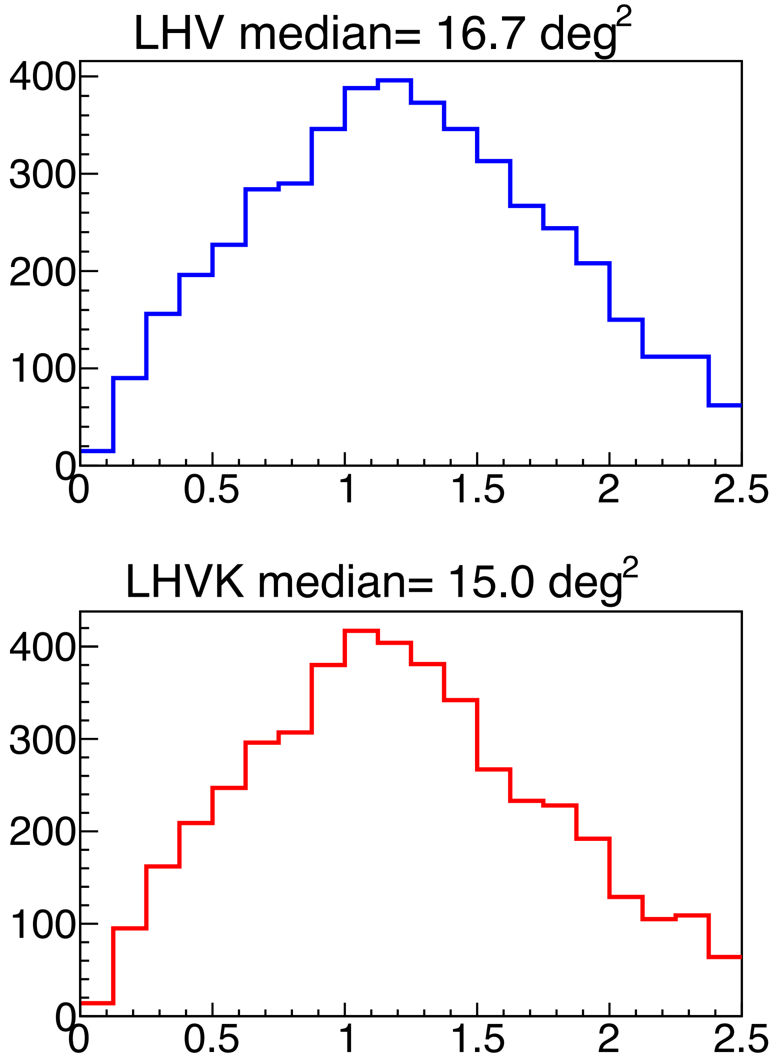

Condition1 : Random inclination

Tagoshi-san's results

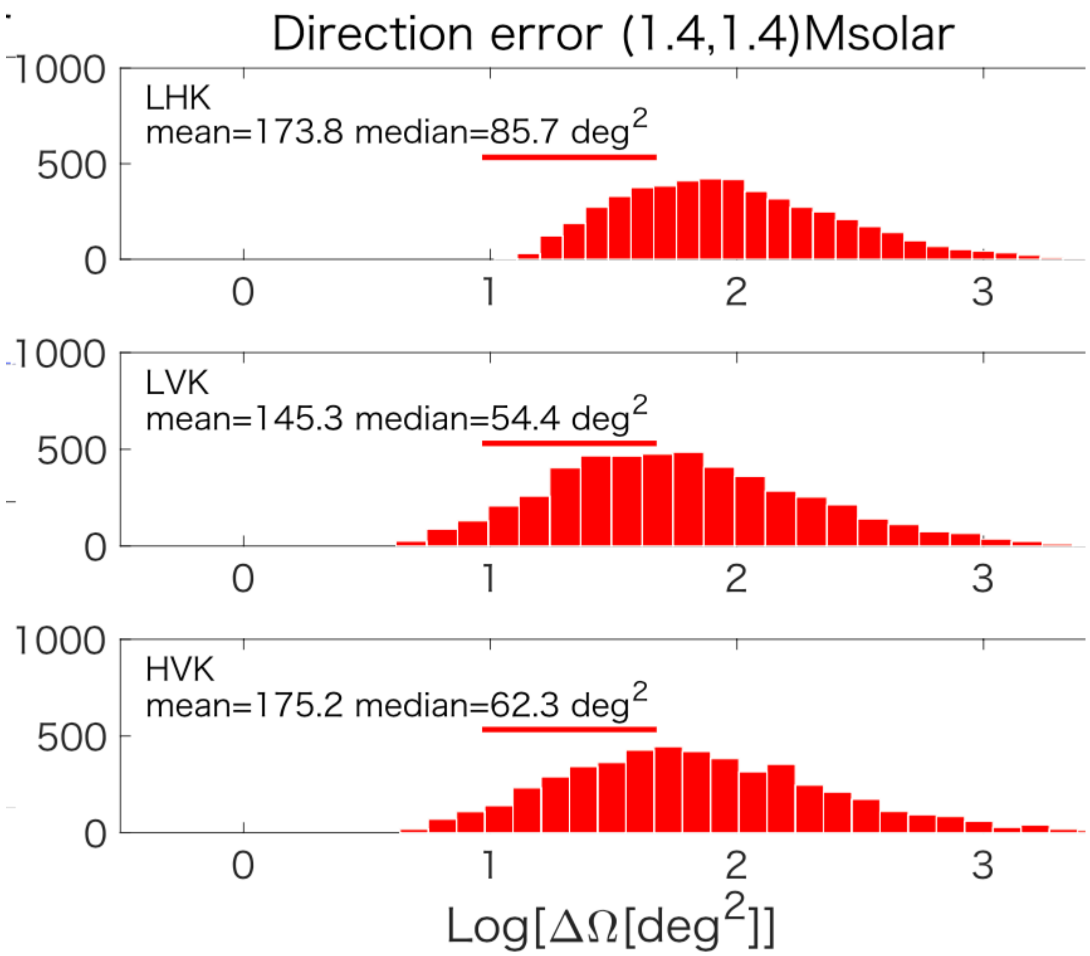

SH

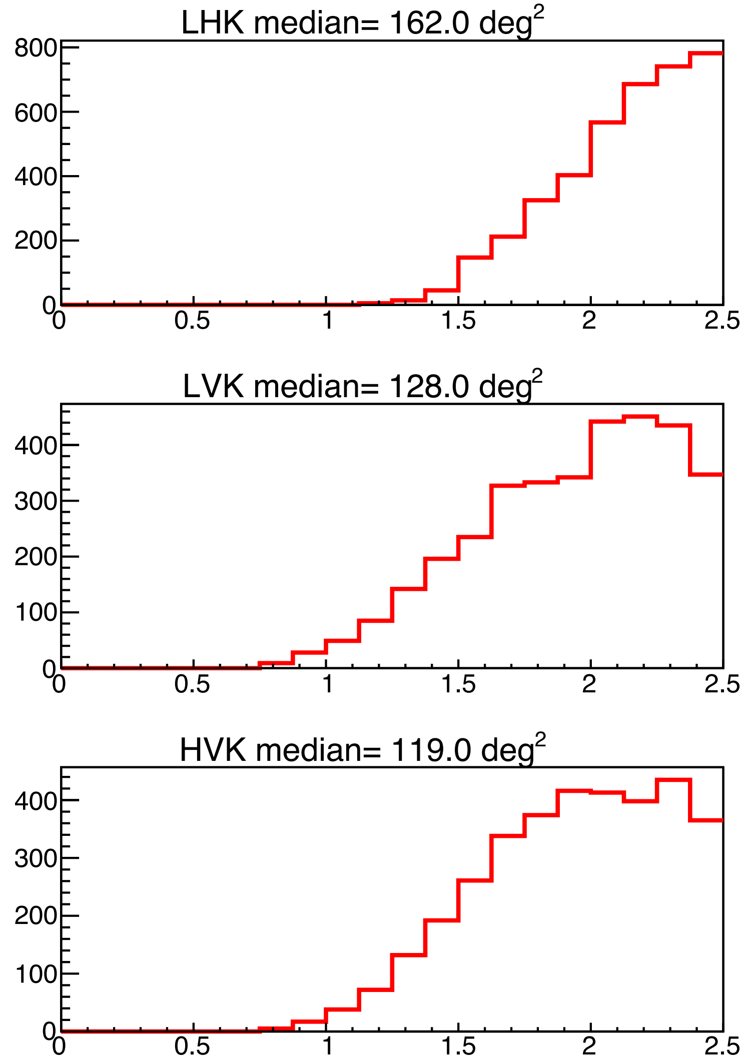

Condition1 : Random inclination

Tagoshi-san's results

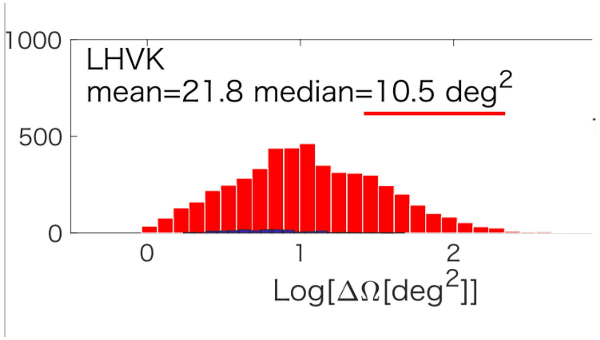

SH

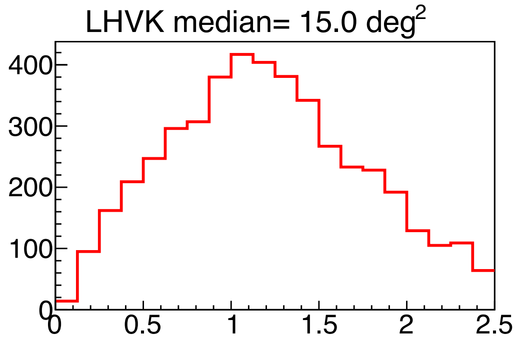

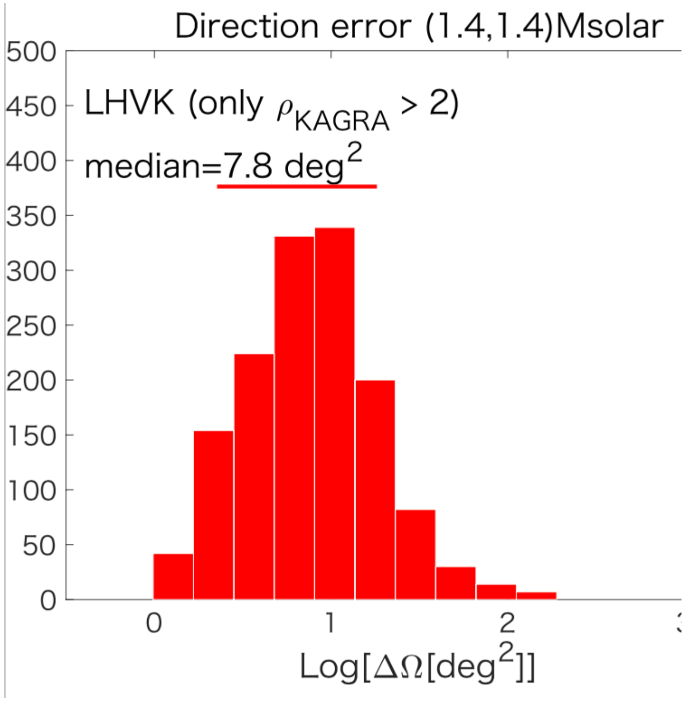

Only ρ_{KAGRA} > 2 cases

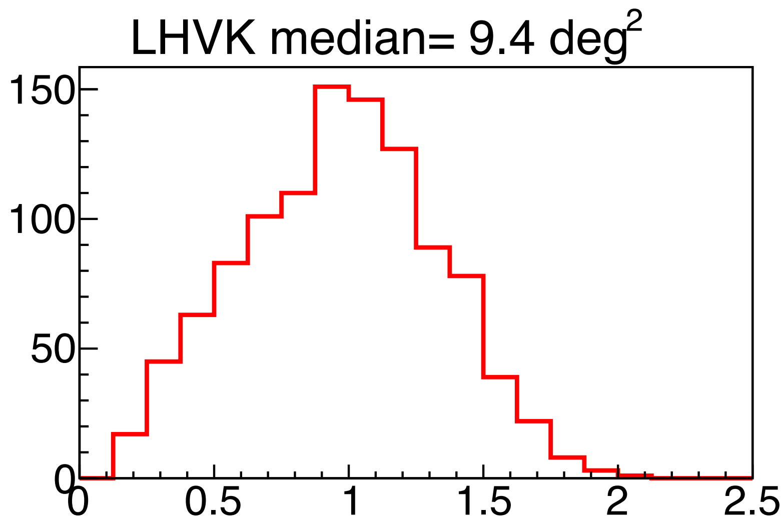

Condition1 : Random inclination

Tagoshi-san's results

Only ρ_{KAGRA} > 2 cases

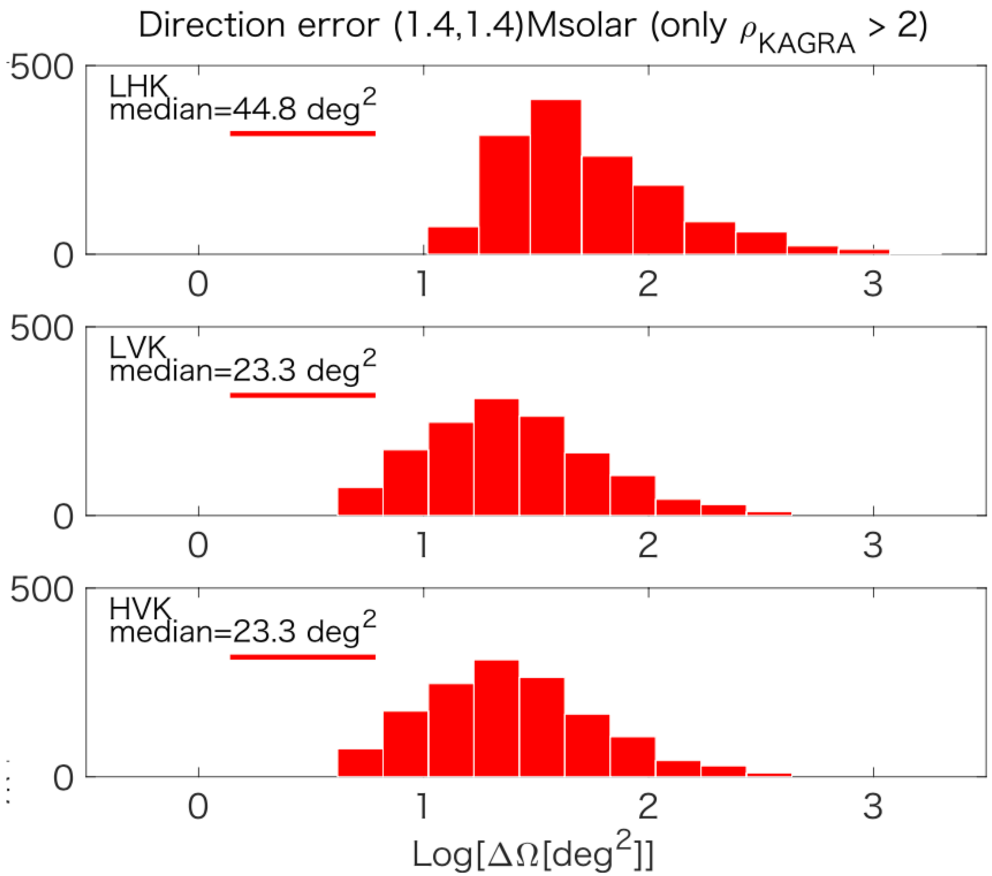

SH

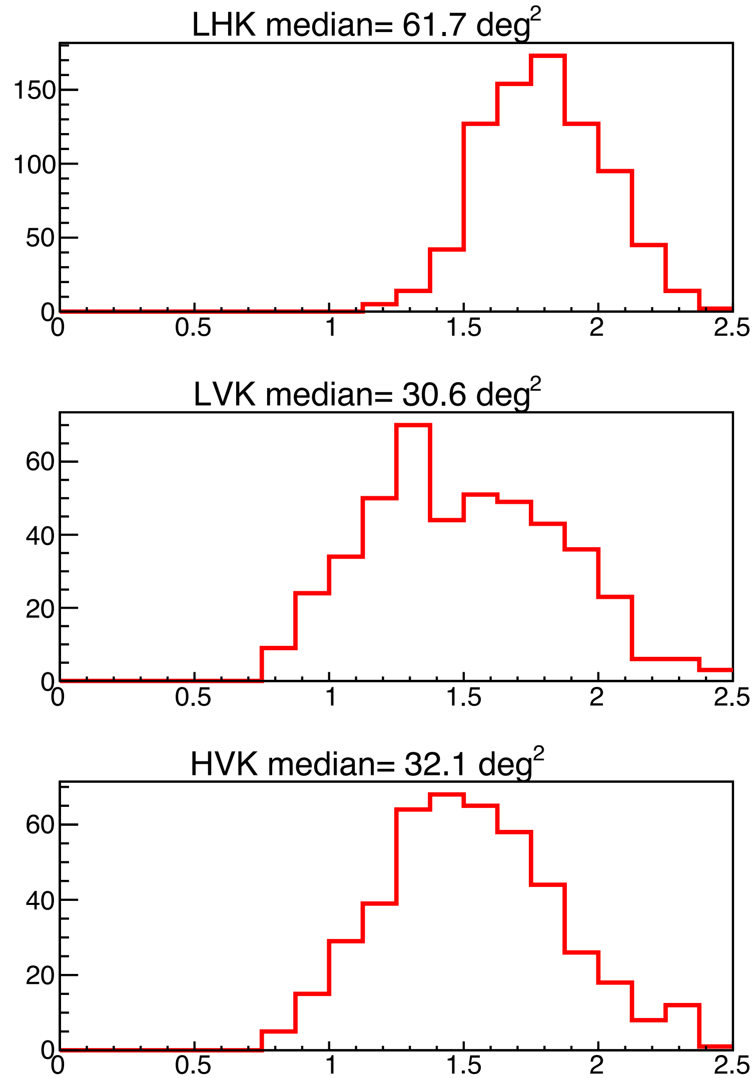

Condition1 : Random inclination

Tagoshi-san's results

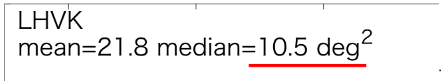

SH

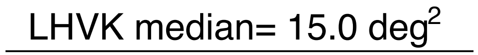

Only ρ_{KAGRA} > 2 cases

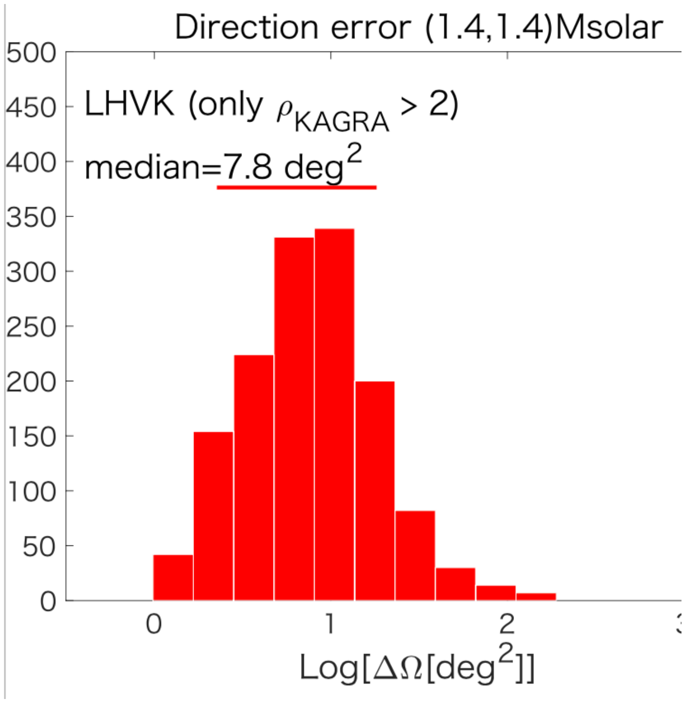

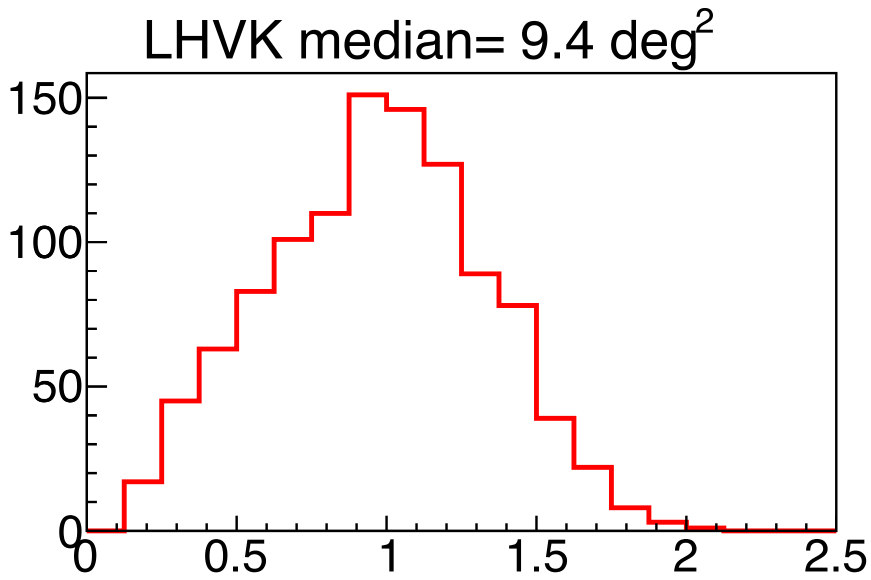

$$\frac{\langle \Delta\Omega_{LHVK}(\rho_{KAGRA} > 2)\rangle}{\langle \Delta\Omega_{\mathrm{LHV}}\rangle} = 0.62$$

$$\frac{\langle \Delta\Omega_{LHVK}(\rho_{KAGRA} > 2)\rangle}{\langle \Delta\Omega_{\mathrm{LHV}}\rangle} = 0.63$$

O3 simulation

Fix distance of BNS at 40 Mpc, then …

- Randomly distribute (BNS: 1.4-1.4)
  - inclination
  - polarization
  - sky location

  (25,000 = 5,000 events x5 detector cases)

- Fix: inclination (4) (BNS: 1.5-1.25)
  and polarization (5)
  - Uniformly distribute source location (192)

  (15,360 = 192 x5 x4 x4 sensitivity cases)

Simulation conditions

Signal injection: NS-NS (1.5-1.25) at 40 Mpc
TaylorF2 waveform (no-spin, no-tidal)

Injected with 15,360 (= 192 x5 x4 x4) conditions:

- 192 (Longitudes and Latitudes – *Healpix* uniform)
- 5 Polarization angles (ψ = 0, 0.2π, 0.4π, 0.6π. 0.8π)
- 4 Inclination angles (θ_{JN} = -30°, -42°, 42°, 30°)
- 4 sensitivity scenarios

computation time for each simulation is ~6 min.
(with GeForce™ GTX 1080 Ti)

Condition2 : Fix inclination

Comparison between Fisher (Y.Michimura et al.) and Nest (SH)

Condition2 : Fix inclination

- LIGO 116 Mpc
- Virgo 62.9 Mpc
- KAGRA 9.5 Mpc

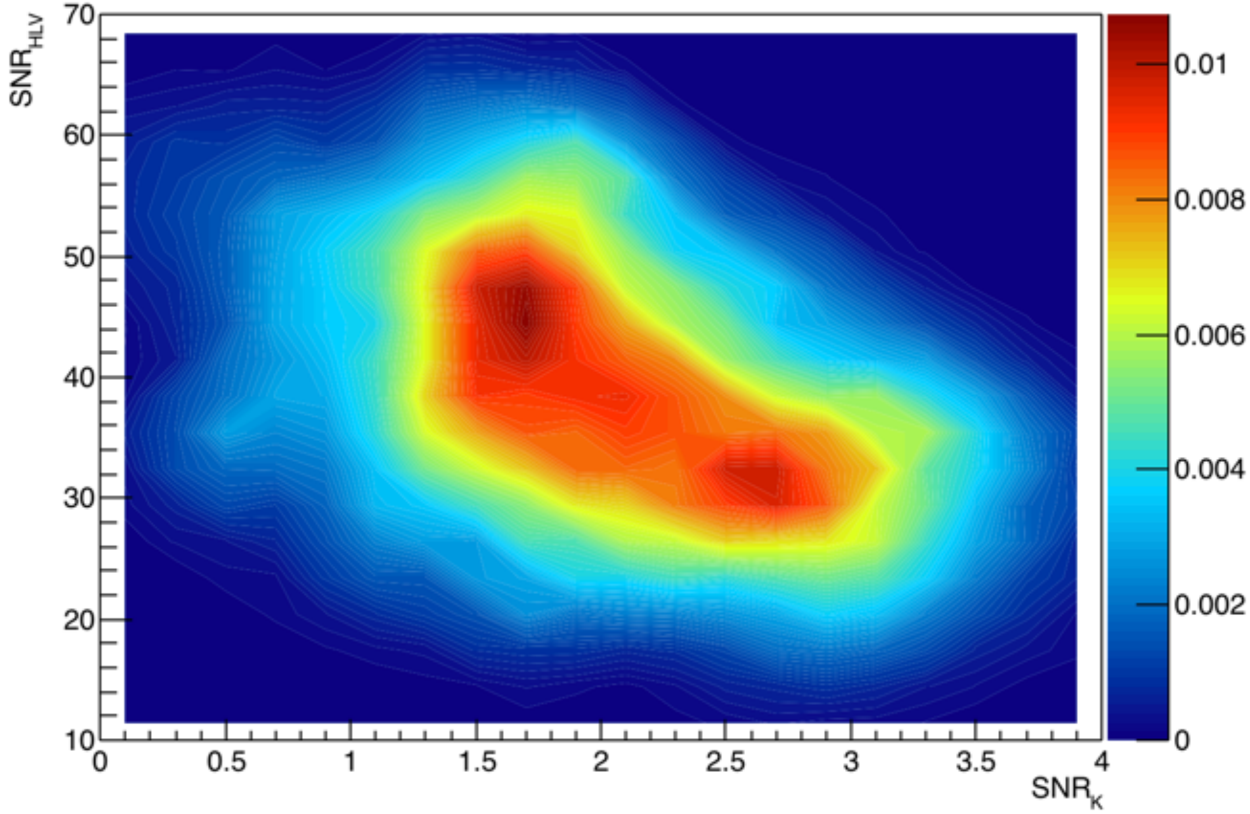

Sensitivity scenarios

	LIGO[*1]	Virgo[*1]	KAGRA[*2]
Case 1	Late Low (116 Mpc)	Mid. Low (62.9 Mpc)	O3-40 (42.3 Mpc)
Case 2	Late Low (116 Mpc)	Late Low (83.1 Mpc)	O3-40 (42.3 Mpc)
Case 3	Late Low (116 Mpc)	Late Low (83.1 Mpc)	O3-20[*3] (20.1 Mpc)
Case 4	Late Low (116 Mpc)	Mid. Low (62.9 Mpc)	O3-10 (9.5 Mpc)

[*1] Sensitivity data from *arXiv:1304.0670* (*LRR 19,1*)
[*2] Sensitivity data by *Y.Enomoto JGW-T1707556*
[*3] Sensitivity data interpolated *JGW-T1707556*

Sky confidence area comparison

Case 1: LVK= 120, 60, 40 M

$\psi = 0$ $\theta_{JN} = 30^{o}$

	LIGO[*1]	Virgo[*1]	KAGRA[*2]
Case 1		~60 Mpc	~40 Mpc
Case 2	~120 Mpc	~80 Mpc	~40 Mpc
Case 3			~20 Mpc
Case 4		~60 Mpc	~10 Mpc

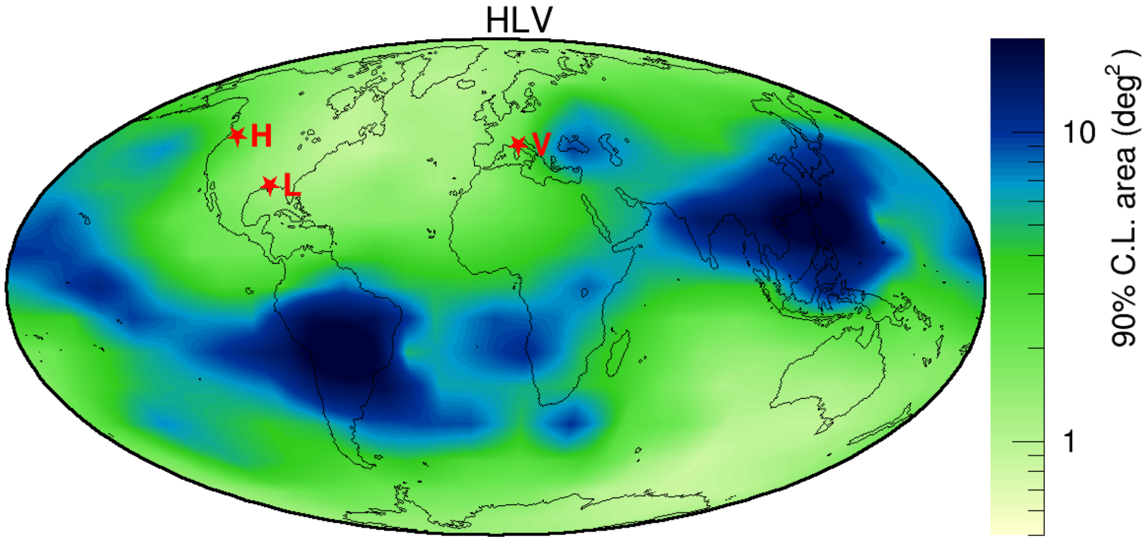

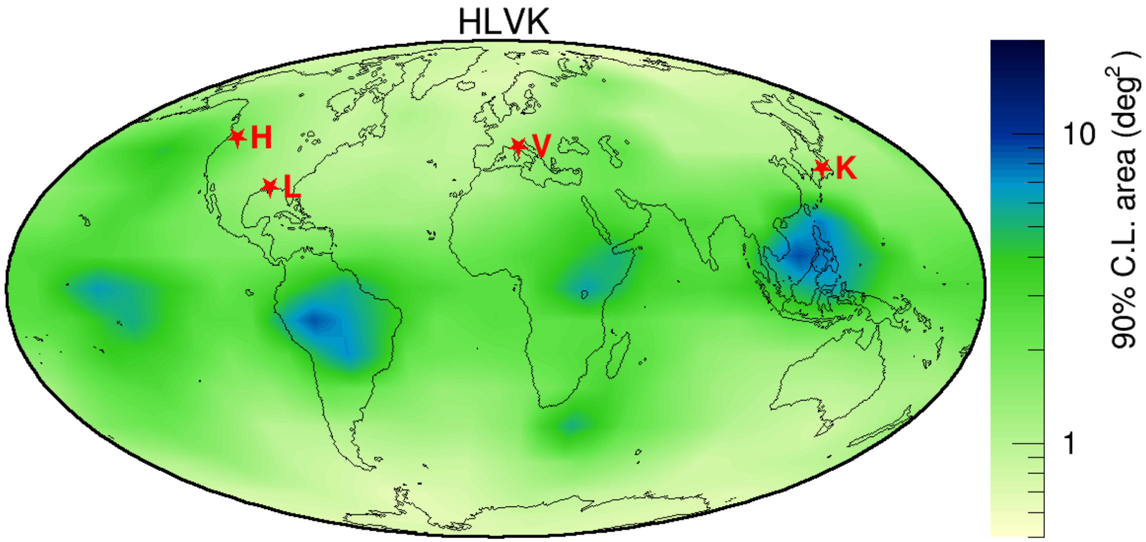

Sky confidence area comparison

Case 1: LVK= 120, 60, 10 Mpc

$\psi = 0$ $\theta_{JN} = 30^{o}$

<table>
<tr><th></th><th>LIGO*1</th><th>Virgo*1</th><th>KAGRA*2</th></tr>
<tr><td>Case 1</td><td rowspan="4">~120 Mpc</td><td>~60 Mpc</td><td>~40 Mpc</td></tr>
<tr><td>Case 2</td><td rowspan="2">~80 Mpc</td><td>~40 Mpc</td></tr>
<tr><td>Case 3</td><td>~20 Mpc</td></tr>
<tr><td>Case 4</td><td>~60 Mpc</td><td>~10 Mpc</td></tr>
</table>

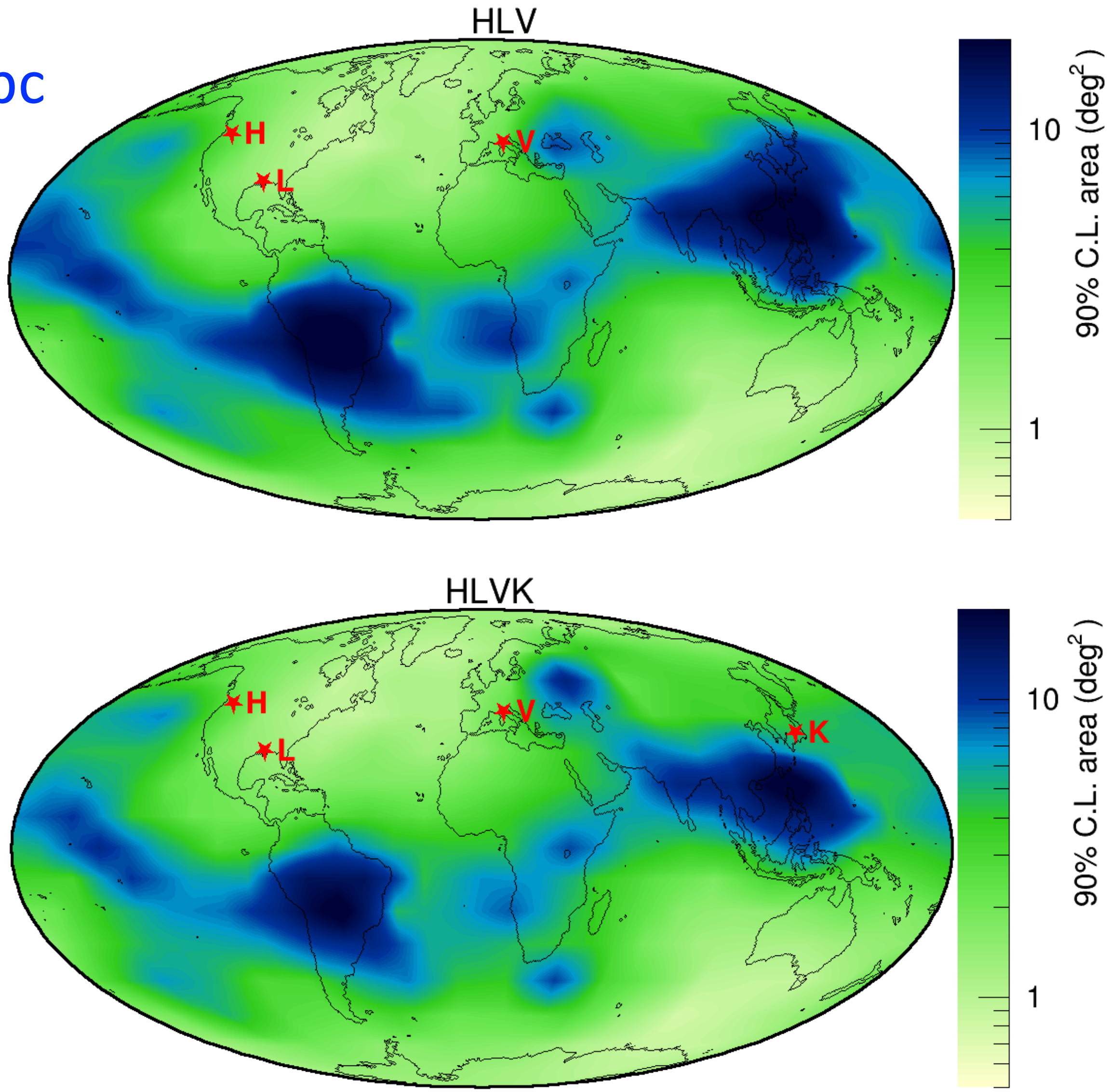

Sky confidence area summary

Averaged over 3840 cases (192 long./lat. 5 ψ, 4 θ_{JN})

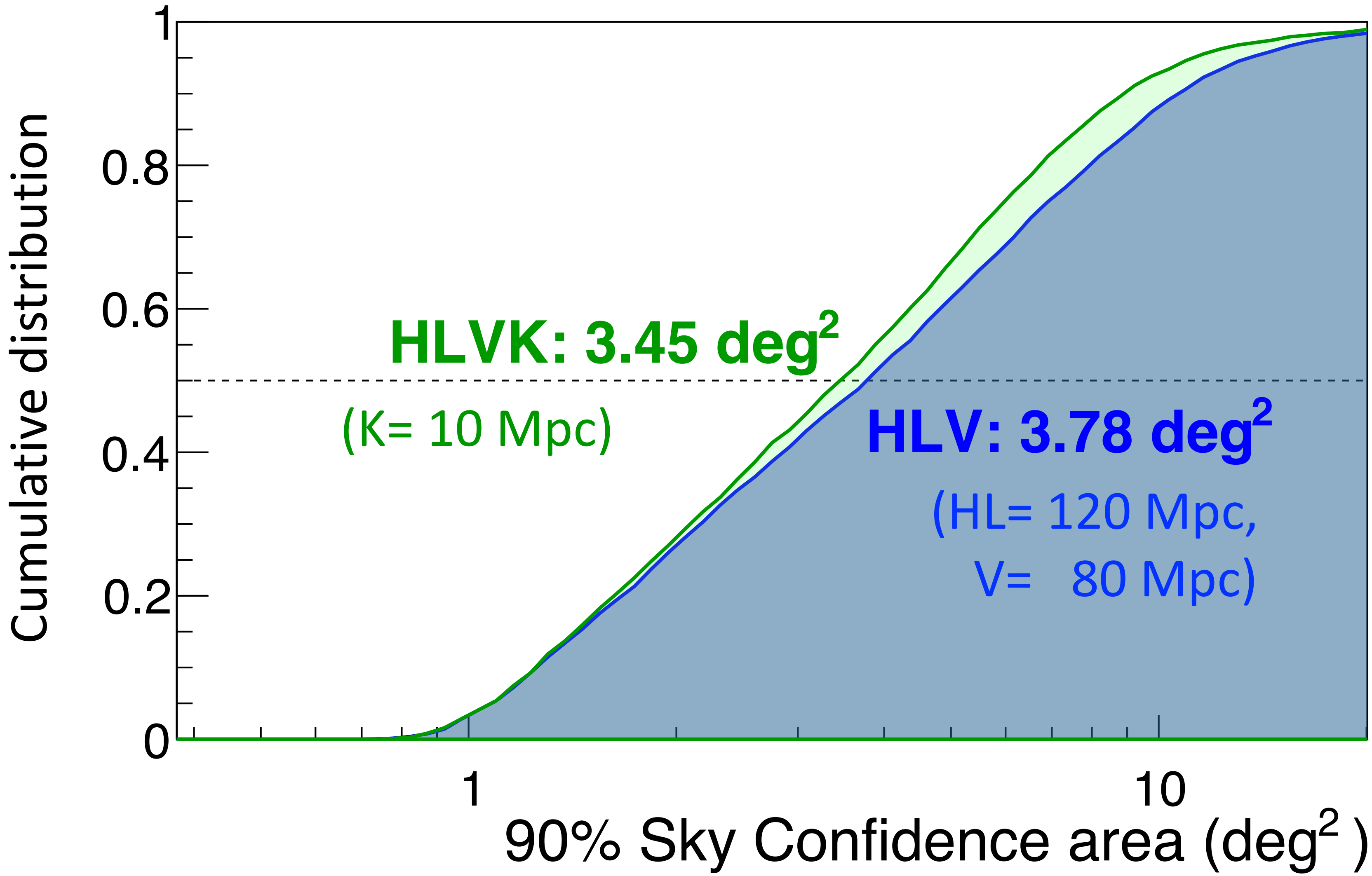

Sky confidence area summary

Averaged over 3840 cases (192 long./lat. 5 ψ, 4 θ_{JN})

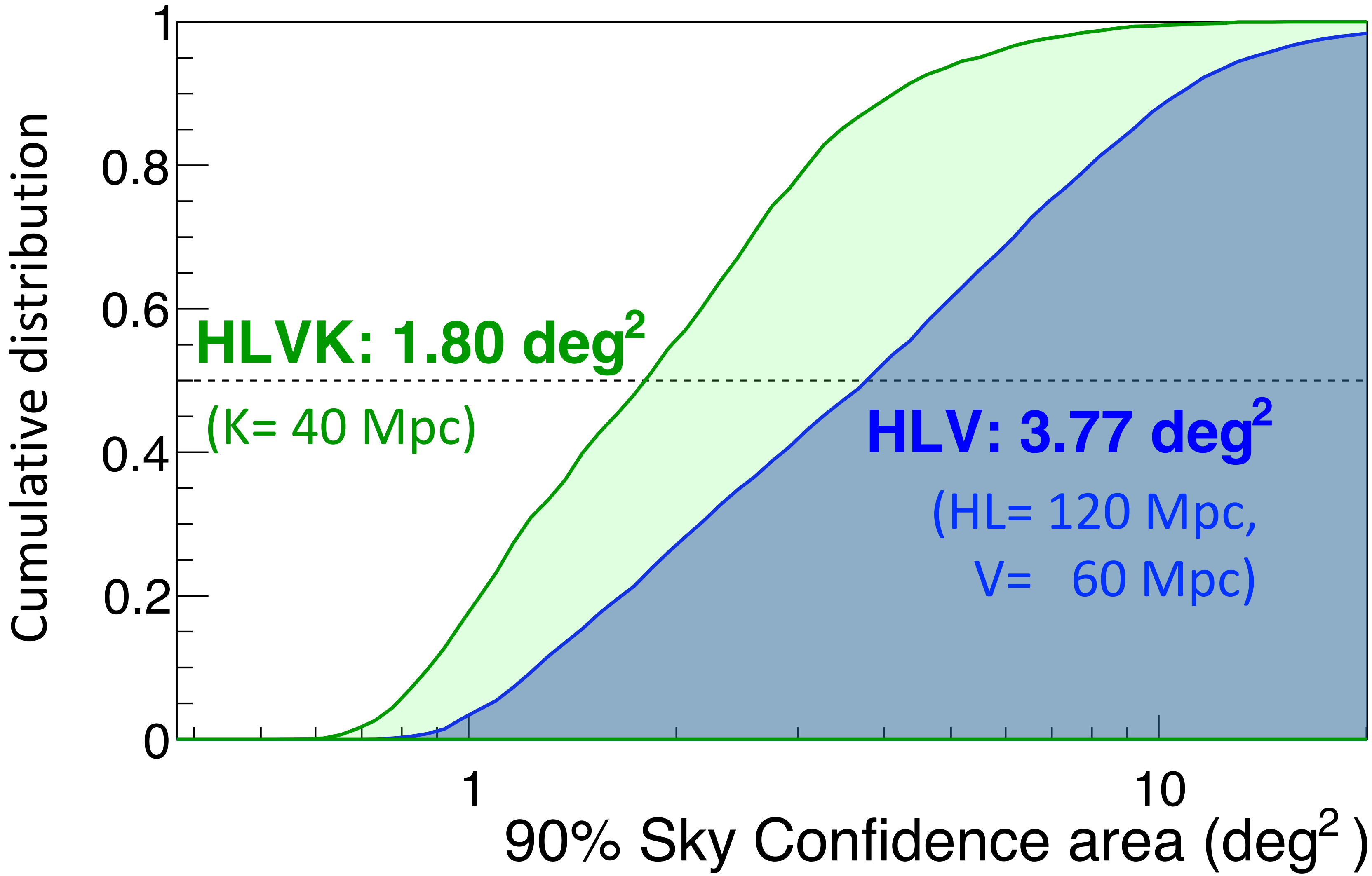

Sky confidence area summary

Averaged over 3840 cases (192 long./lat. 5 ψ, 4 θ_{JN})

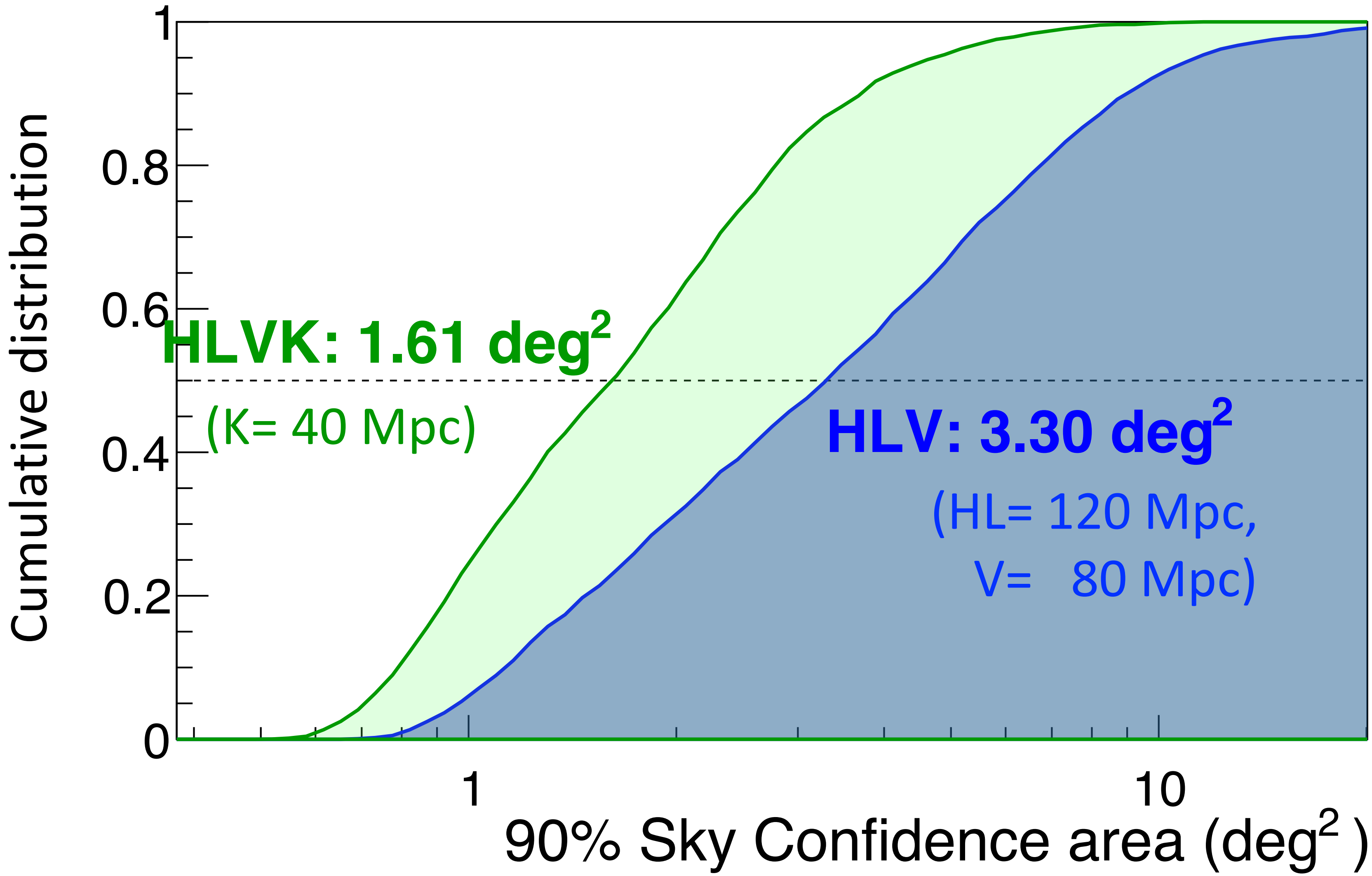

Sky confidence area summary

Averaged over 3840 cases (192 long./lat. 5 ψ, 4 θ_{JN})

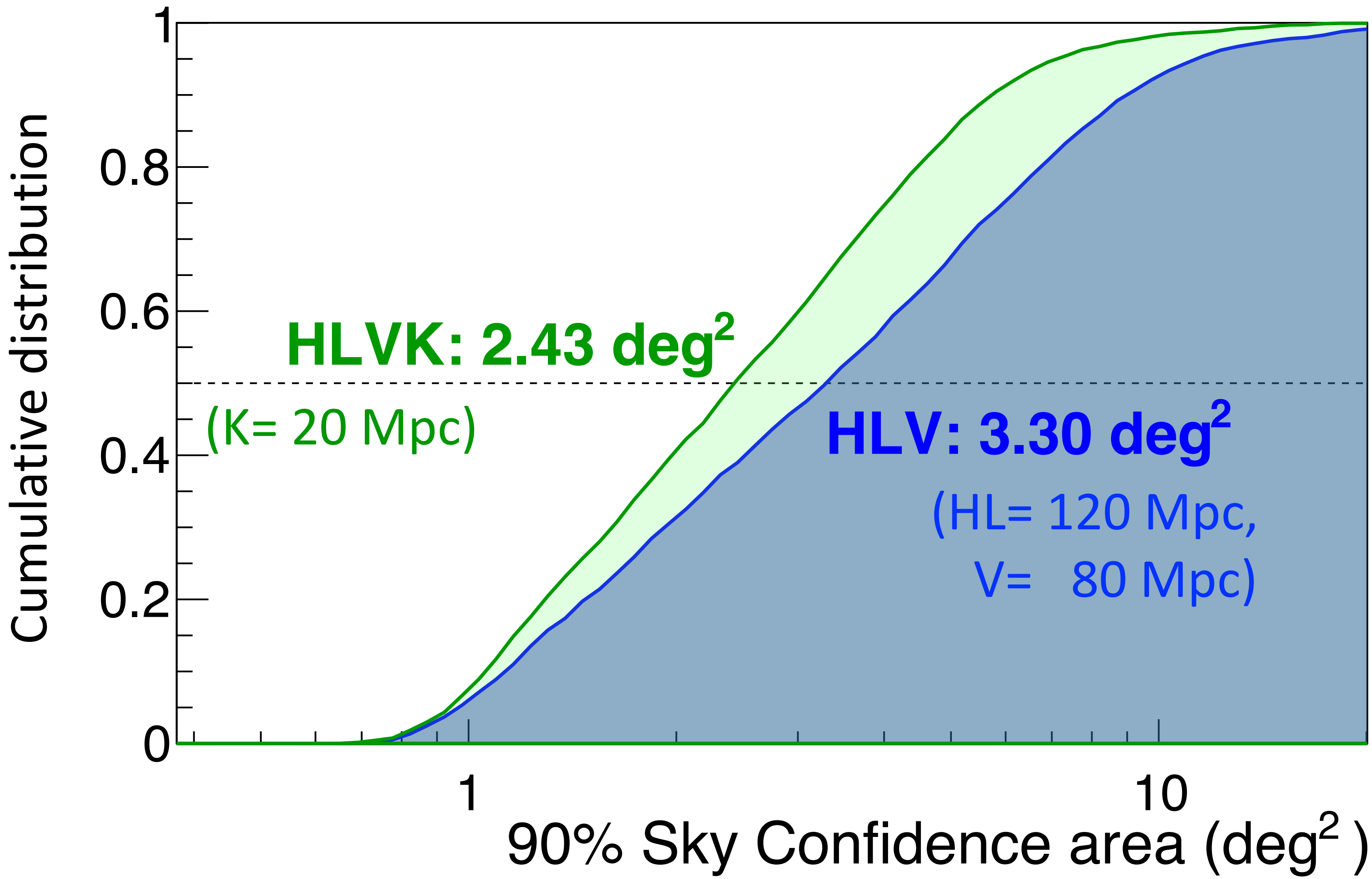

Distance estimation error

Averaged over 3840 cases (192 long./lat. 5 ψ, 4 θ_{JN})

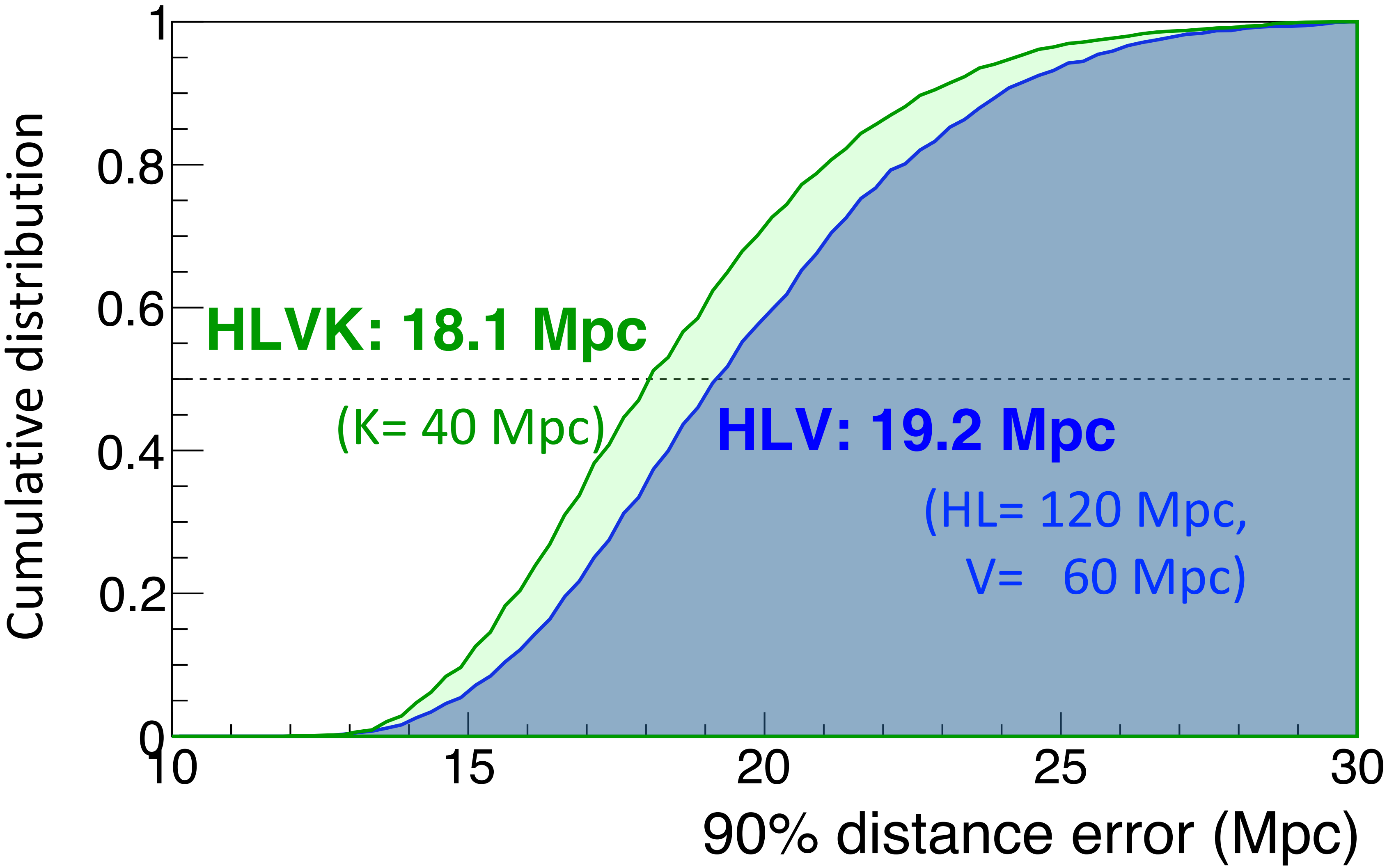

Inclination angle estimation error

Averaged over 3840 cases (192 long./lat. 5 ψ, 4 θ_{JN})

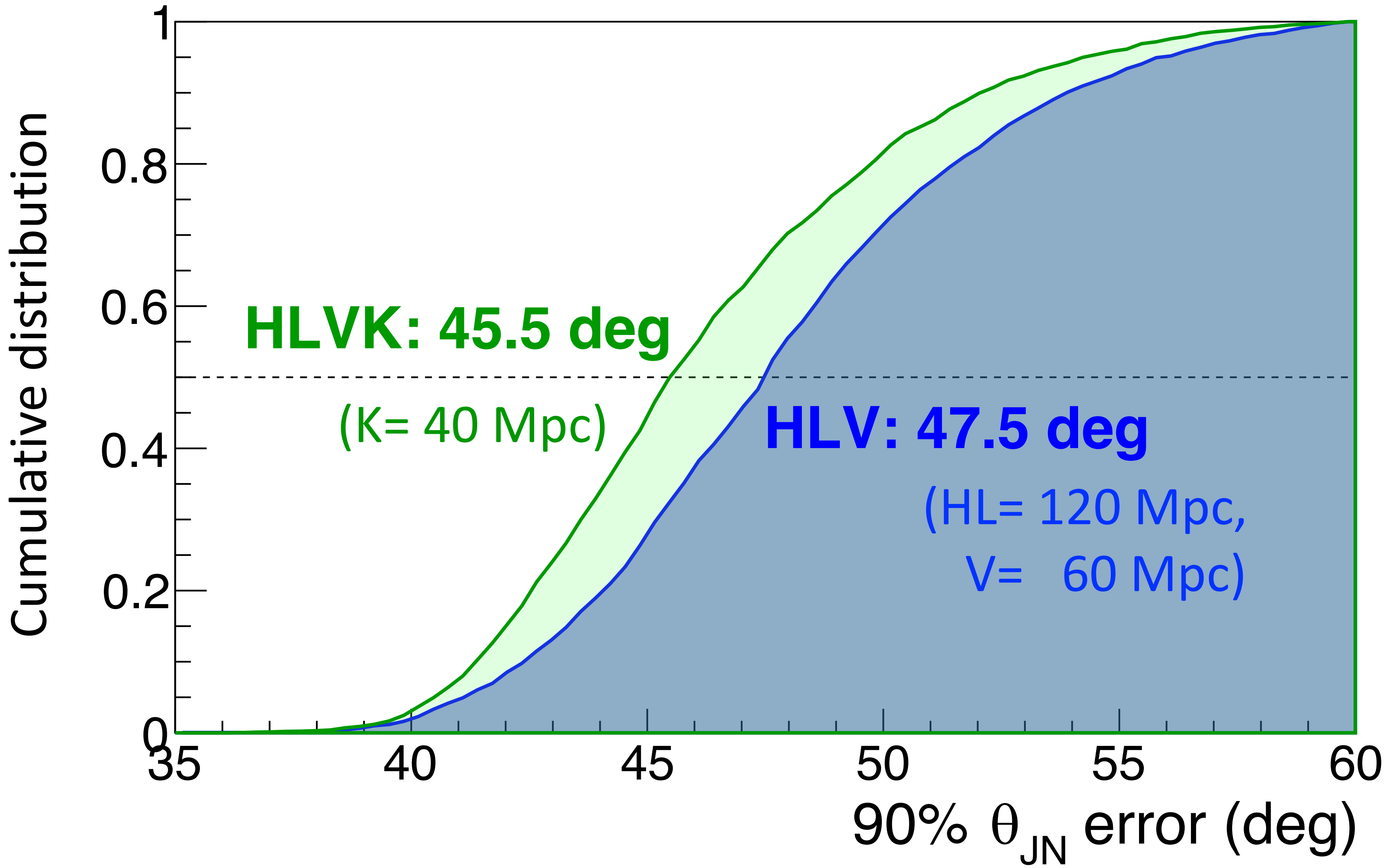

Simulation results

http://www.icrr.u-tokyo.ac.jp/~haino/gsim/gsim.html

LVK (LIGO-Virgo-KAGRA) simulation results

Mass	Distance	LIGO	Virgo	KAGRA	Summary	Sky map
1.5-1.25 MS	40 Mpc	120 Mpc	60 Mpc	40 Mpc	[+] Expand	[+] Expand
1.5-1.25 MS	40 Mpc	120 Mpc	60 Mpc	10 Mpc	[+] Expand	[+] Expand
1.5-1.25 MS	40 Mpc	120 Mpc	80 Mpc	40 Mpc	[+] Expand	[+] Expand
1.5-1.25 MS	40 Mpc	120 Mpc	80 Mpc	20 Mpc	[+] Expand	[+] Expand
1.5-1.25 MS	40 Mpc	120 Mpc	80 Mpc	10 Mpc	[+] Expand	[+] Expand
1.5-1.25 MS	10 Mpc	120 Mpc	60 Mpc	40 Mpc		[+] Expand

Updated by S.Haino on Mar 20, 2018

Refs: JGW-G1807674 JGW-G1808042

Simulation results

http://www.icrr.u-tokyo.ac.jp/~haino/gsim/gsim.html

LVK (LIGO-Virgo-KAGRA) simulation results

Mass	Distance	LIGO	Virgo	KAGRA	Summary	Sky map
1.5-1.25 MS	40 Mpc	120 Mpc	60 Mpc	40 Mpc	[-] Collapse	[+] Expand

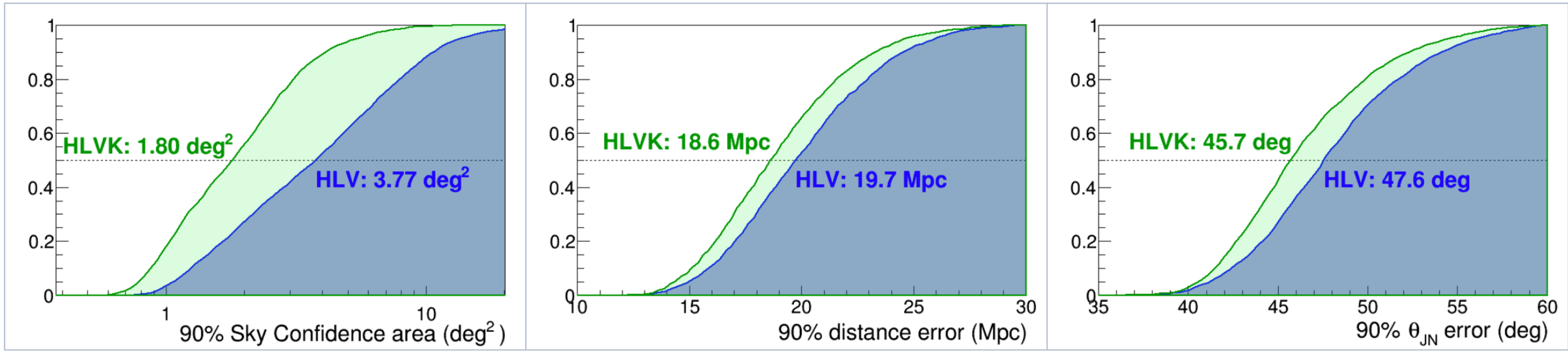

Data (HLV)

Data (HLVK)

Mass	Distance	LIGO	Virgo	KAGRA	Summary	Sky map
1.5-1.25 MS	40 Mpc	120 Mpc	60 Mpc	10 Mpc	[+] Expand	[+] Expand
1.5-1.25 MS	40 Mpc	120 Mpc	80 Mpc	40 Mpc	[+] Expand	[+] Expand
1.5-1.25 MS	40 Mpc	120 Mpc	80 Mpc	20 Mpc	[+] Expand	[+] Expand
1.5-1.25 MS	40 Mpc	120 Mpc	80 Mpc	10 Mpc	[+] Expand	[+] Expand
1.5-1.25 MS	10 Mpc	120 Mpc	60 Mpc	40 Mpc		[+] Expand

O3 simulation

Fix distance of BNS at 40 Mpc, then …

- Randomly distribute
  Significant improvement even with 10 Mpc
  (By selecting ρ_K>2)

$$\frac{\langle \Delta\Omega_{LHVK}(\rho_{KAGRA} > 2)\rangle}{\langle \Delta\Omega_{\mathrm{LHV}}\rangle} = 0.62$$

- Fix: inclination and polarization
  Only a small improvement with 10 Mpc
  > 20 Mpc
  is required

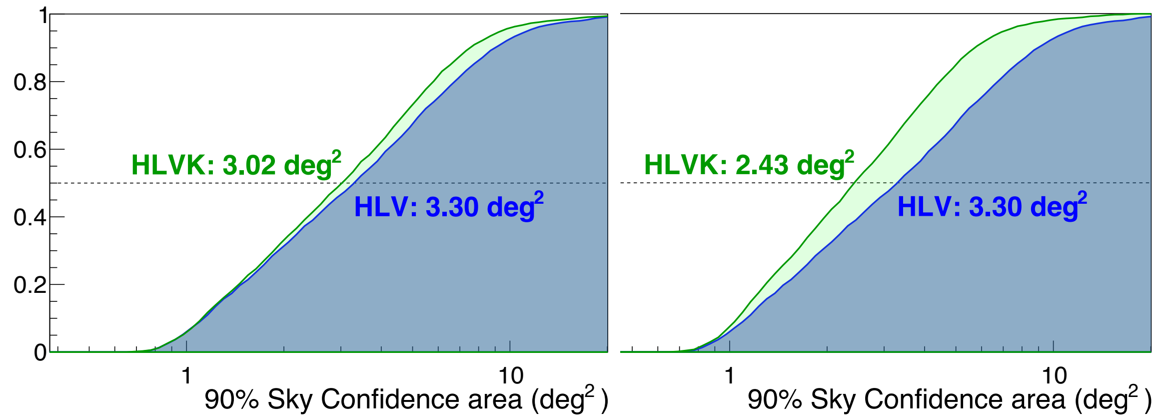

Outline

- G.P.E. – GPU accelerated Parameter Estimation
- Comparison of results – GW events analysis
- Comparison of results – Simulation
- Immediate future – O3 simulation
- Physics targets – O5 simulation

Outline

- G.P.E. – GPU accelerated Parameter Estimation
- Comparison of results – GW events analysis
- Comparison of results – Simulation
- Immediate future – O3 simulation
- Physics targets – O5 simulation

KAGRA physics targets (O5)

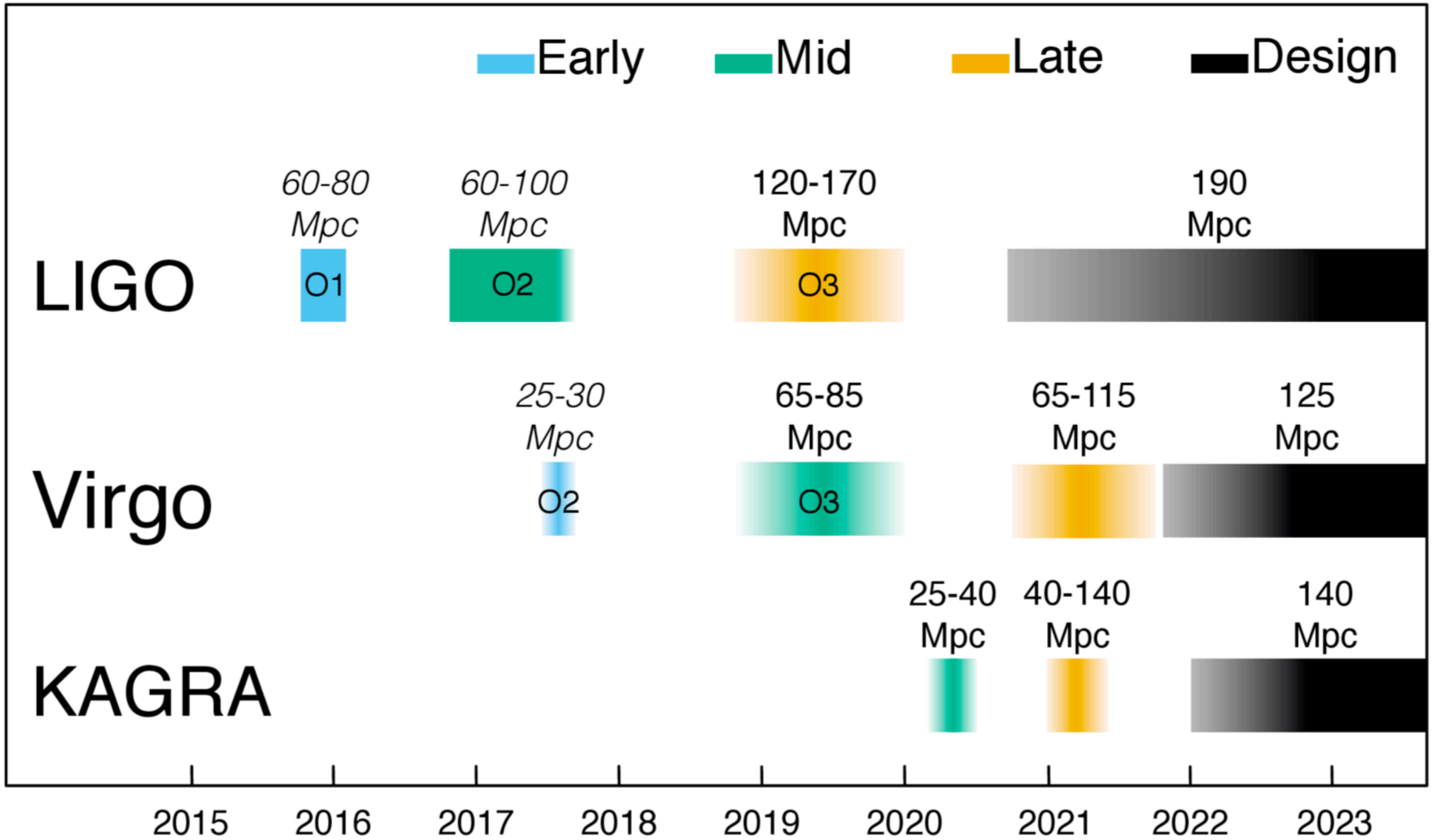

Physics example:

Hubble constant
– an issue and a new hope

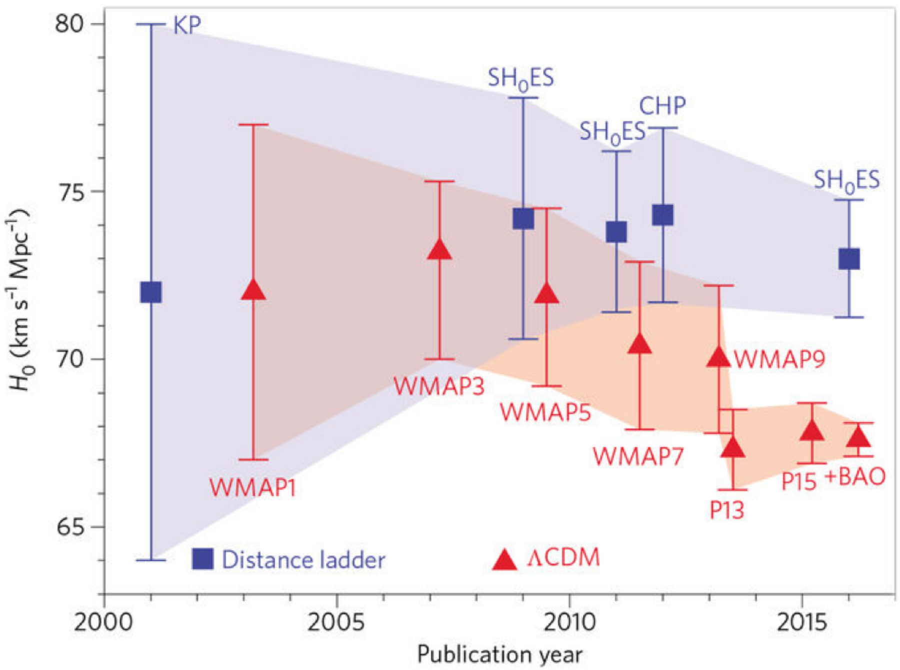

Nature Astronomy **1**, 0121 (2017)

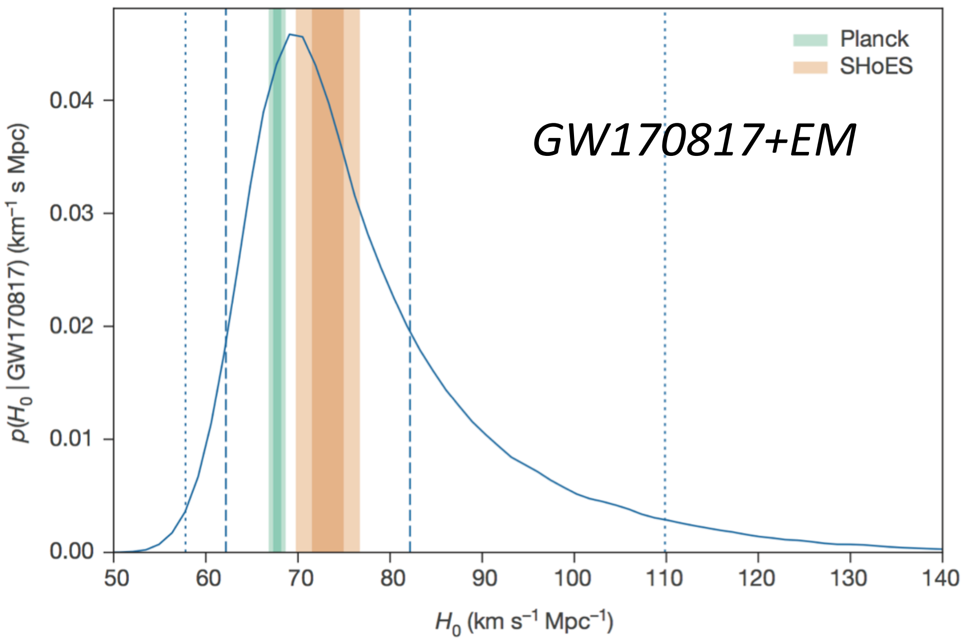

Nature **551**, 85 (2017)

GW standard siren (BNS, NSBH?)

- GW => Luminosity distance
  EM => redshift

- Good sky localization is needed to identify EM (Ndet >= 3)

- By accumulating many BNS events,
  distance error can be reduced with sqrt(N)

KAGRA’s contribution

KAGRA (with design sensitivity) will improve

- Network SNR
- Effective duty cycle (3/4 >> 3/3)
- Sky localization
- Distance/inclination estimation
- …

BNS simulation

- 10,000 events with random distributions of
  - mass (1.0 – 2.0 Ms)
  - distance (by volume)
  - inclination, polarization, sky location
- Assuming design sensitivity

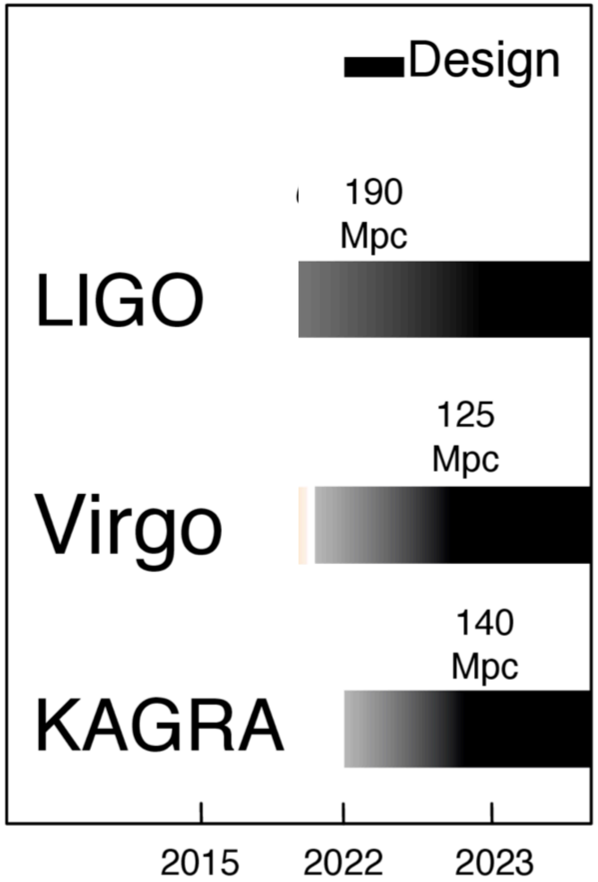

Hubble constant from GW siren

$$c\,z = v^{\rm p} + H_0\,d.$$

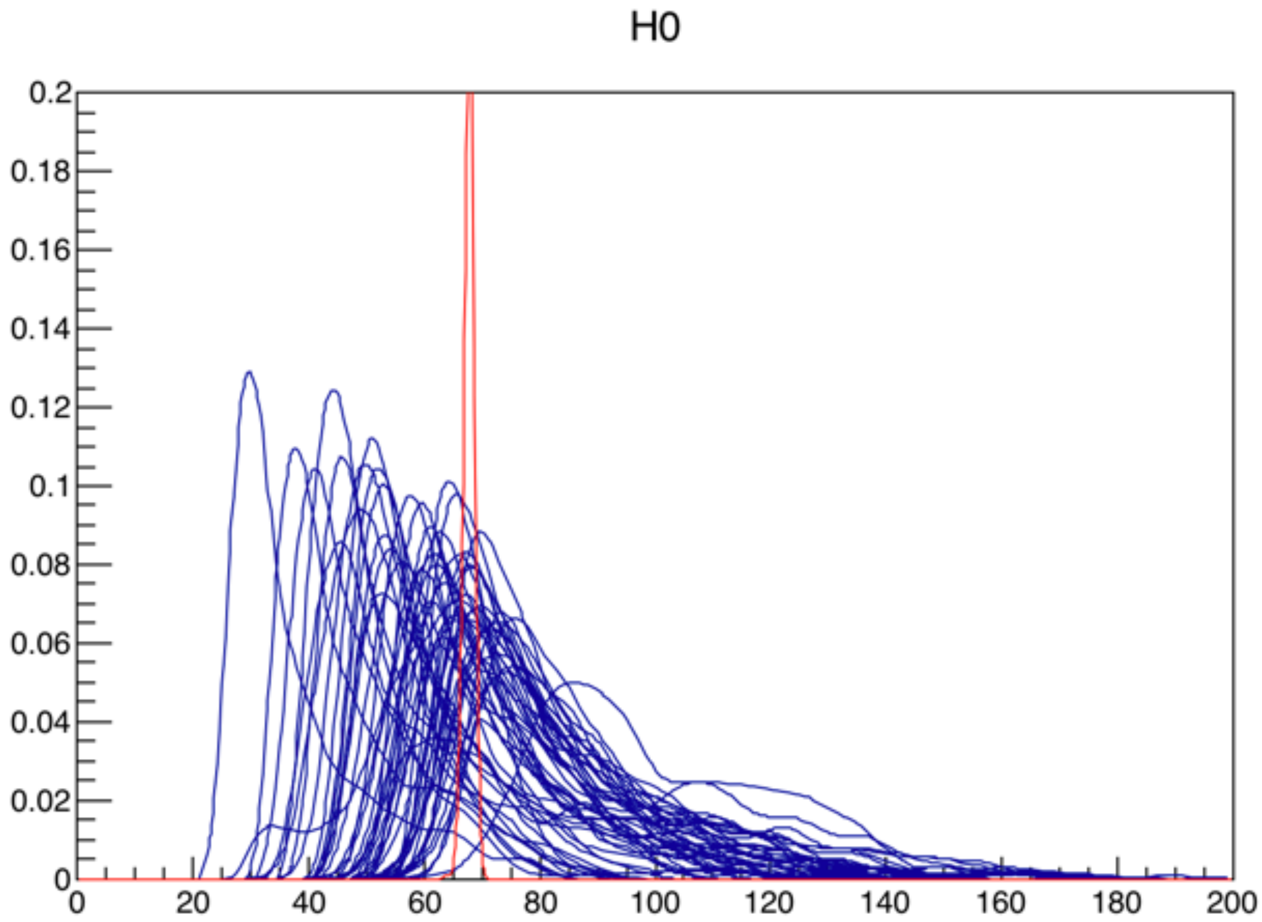

Hubble constant VS events

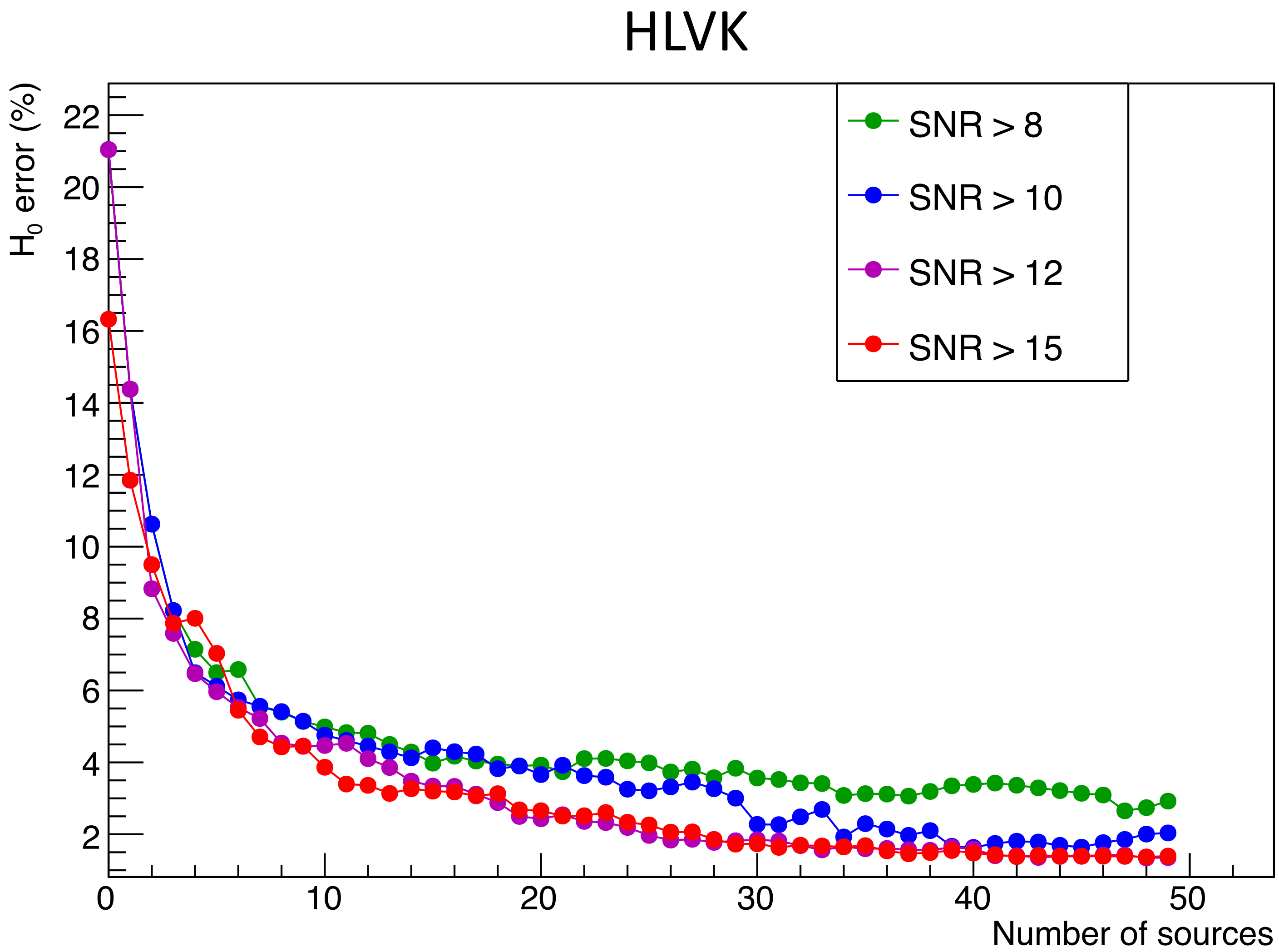

Hubble constant error VS time

Assumed duty cycle : 80% for each detector

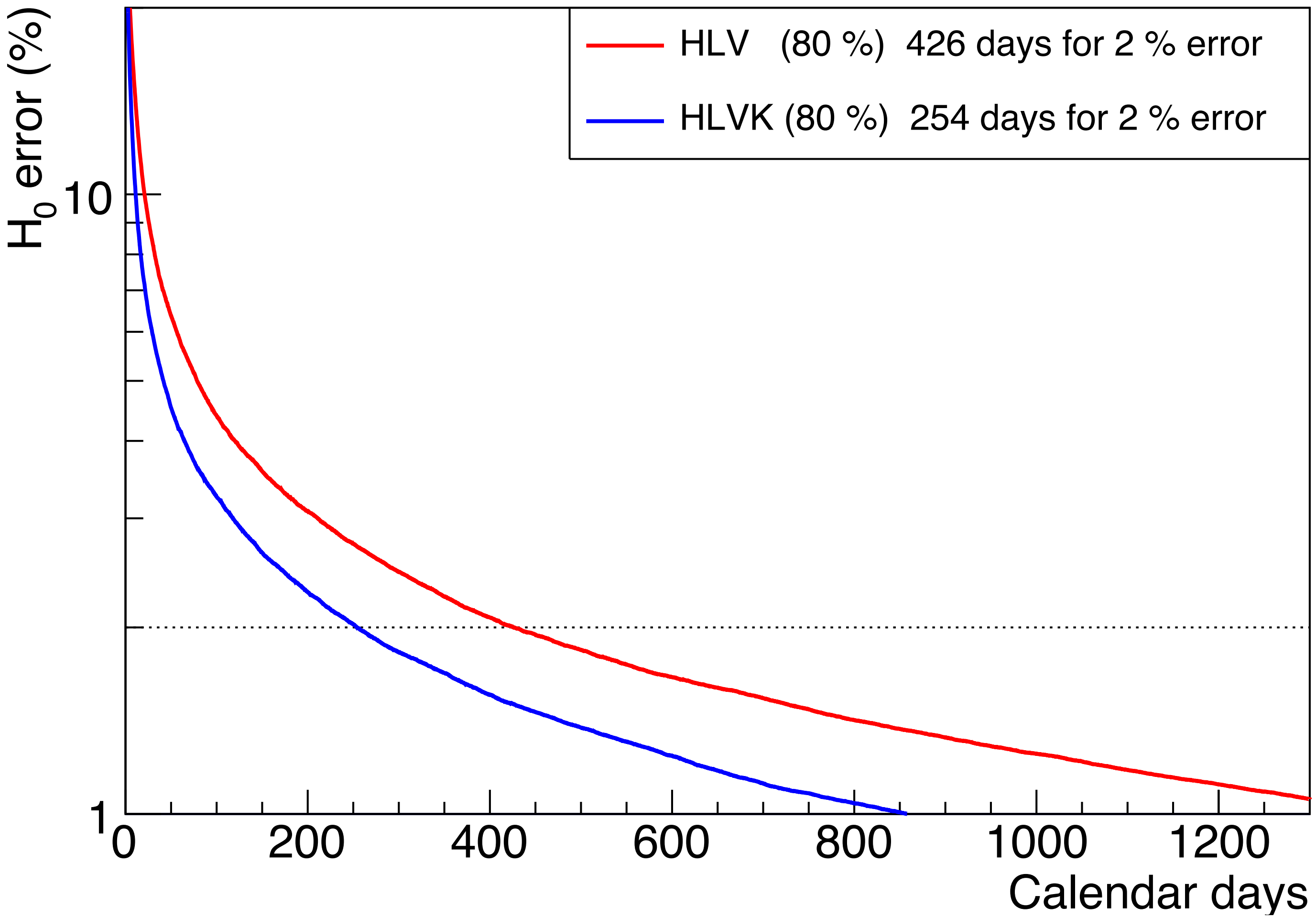

Hubble constant error VS time

Assumed duty cycle : 60% for each detector

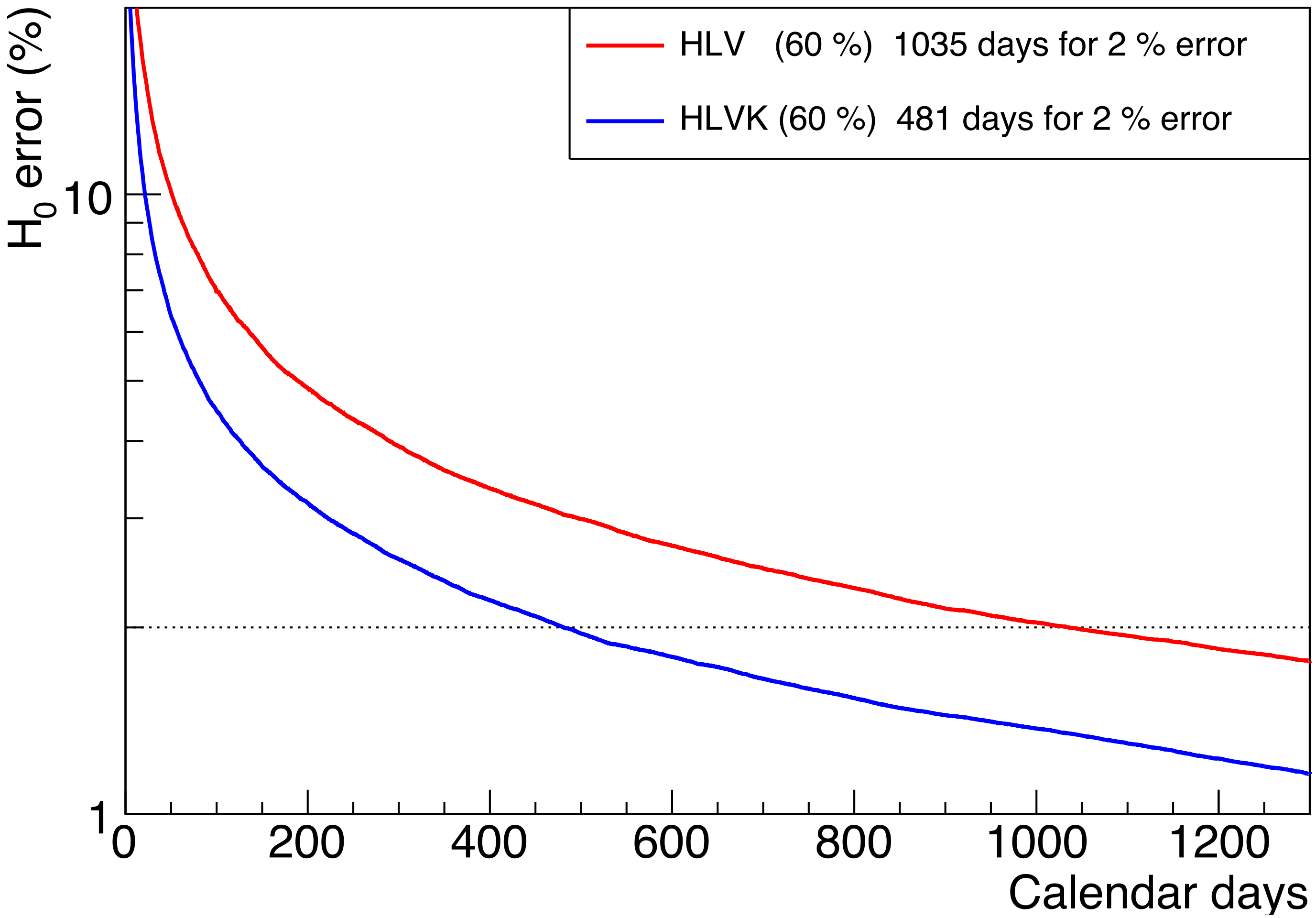

NSBH

arXiv1804.07337

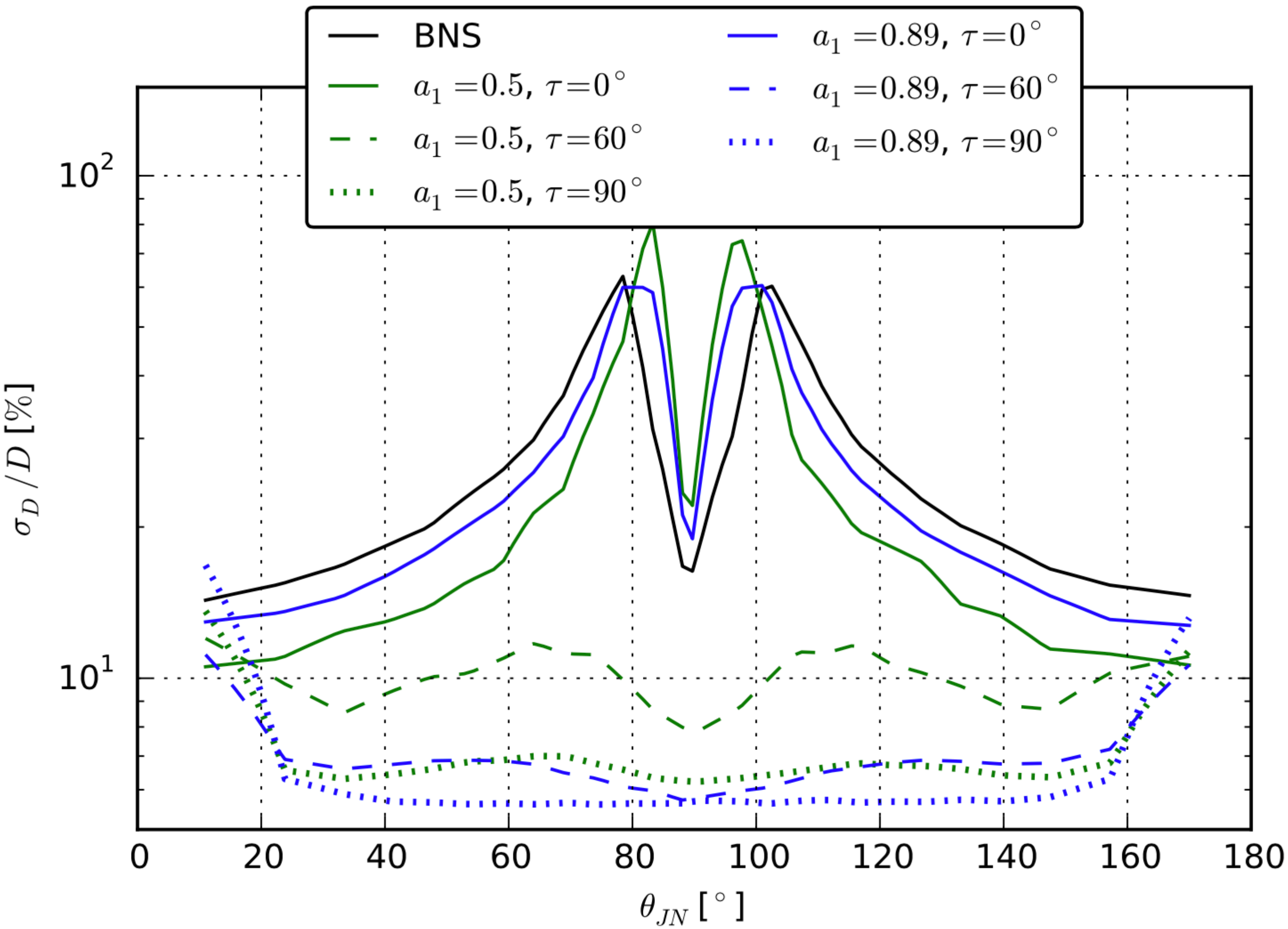

KAGRA physics targets (O5)

- To be continued…

- More detailed discussions expected in KSC session of the coming f2f meeting at OCU

14:45-16:30	Session 15: **KSC and Collaborators session** (Chair: xxxx)	
	R&D authorization ()	Yoichi Aso (NAOJ)
	Phase-1 paper (15min)	??
	KAGRA physics targets (20min)	Sadakazu Haino (Academia Sinica)
	CPC (5 min)	??
	Default Author-List 2017 (5 min)	Hisaaki Shinkai (Osaka Inst. Tech.)
	Document and Drawing ()	??

Another on-going project

- Evaluating calibration error by implementing realistic IFO model and calibration error priors
- To be discussed in Kiban(s) meeting (May/21 OCU)

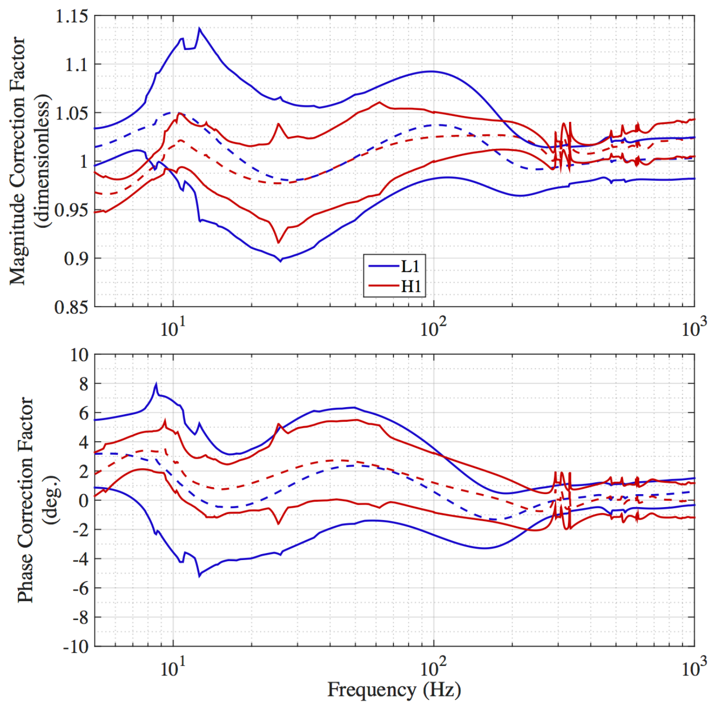

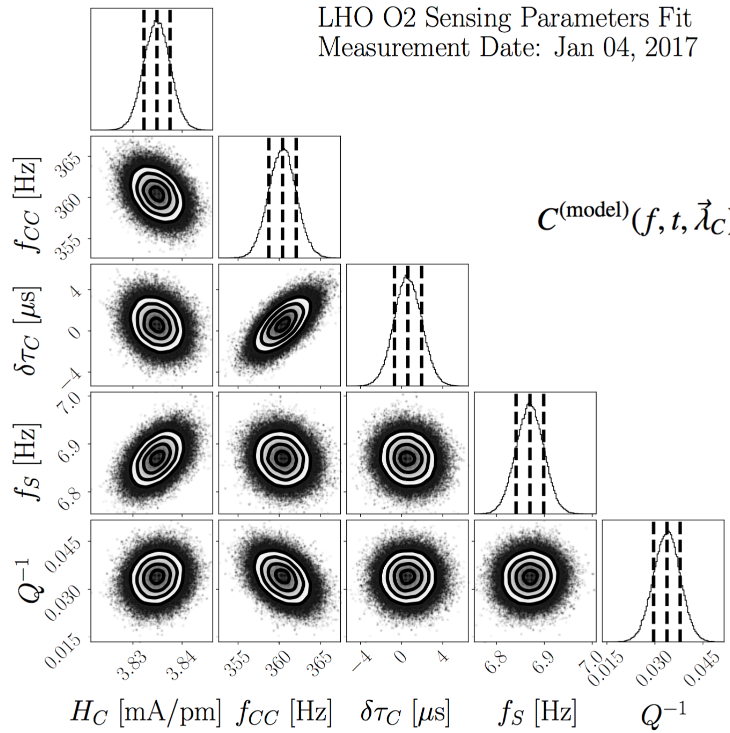

$$C^{(\mathrm{model})}(f,t,\vec{\lambda}_C) = \frac{\kappa_C(t)\,H_C}{1+if/f_{CC}}\,C_R(f)\,e^{2\pi i f \tau_C} \times \frac{f^2}{f^2+f_S^2-iff_S Q_S^{-1}}$$